Mesoporous Silica Nanoparticles: Synthesis, Biocompatibility and Drug Delivery

Fangqiong Tang, Linlin Li, and Dong Chen*

In the past decade, mesoporous silica nanoparticles (MSNs) have attracted more and more attention for their potential biomedical applications. With their tailored mesoporous structure and high surface area, MSNs as drug delivery systems (DDSs) show significant advantages over traditional drug nanocarriers. In this review, we overview the recent progress in the synthesis of MSNs for drug delivery applications. First, we provide an overview of synthesis strategies for fabricating ordered MSNs and hollow/rattle-type MSNs. Then, the in vitro and in vivo biocompatibility and biotranslocation of MSNs are discussed in relation to their chemophysical properties including particle size, surface properties, shape, and structure. The review also highlights the significant achievements in drug delivery using mesoporous silica nanoparticles and their multifunctional counterparts as drug carriers. In particular, the biological barriers for nano-based targeted cancer therapy and MSN-based targeting strategies are discussed. We conclude with our personal perspectives on the directions in which future work in this field might be focused.

1. Introduction

Since the first report using MCM-41 type mesoporous silica nanoparticles (MSNs) as drug delivery system in 2001,[1] the last ten years have witnessed an exponential increase in research on biomedical application of MSNs (**Figure 1**). It has been one the hottest areas in nanobiotechnology and nanomedicine for designing biocompatible MSNs and multifunctional counterparts in disease diagnosis and therapy. As nanocarriers, mesoporous silica nanoparticles with unique mesoporous structure have been explored as effective drug delivery systems for a variety of therapeutic agents to fight against various kinds of diseases including bone/tendon tissue engineering,[2–5] diabetes,[6,7] inflammation,[8] and cancer.[9] Through much effort MSNs have been proven to possess unprecedented advantages over traditional nano-based formulations, especially for cancer therapy.

The worldwide research interest in biomedical applications of MSNs should mainly be attributed to the gradually increased requirements from clinical patients for high-performance therapeutic nanoformulations. MSNs as nanometer-sized drug carriers are expected to overcome some of the problems of current nanoformulations. Therapeutic nanoformulations have been marketed from the mid-1990s.[10,11] Unfortunately, great efforts and vast investments over the past thirty years have yielded only a few nanoformulations that were approved by the US Food and Drug Administration (FDA) for clinical applications such as Doxil (100-nm PEGylated (polyethylene glycol coated) liposome encapsulating doxorubicin hydrochloride, which was approved by FDA in 1995 for treatment of refractory Kaposi's sarcoma, recurrent breast cancer and ovarian cancer) and Abraxane (albumin-bound paclitaxel with a mean particle size of approximately 130 nm, which was approved by the FDA in 2005 for metastatic breast cancer). From a scientific point of view, there have several key barriers blocking the clinical translocation of laboratory-developed nanoformulations.[12–14] The first major hurdle is the difficulty to develop nanocarriers that encapsulate sufficient therapeutic agents with activated release. Second, it is difficult to deliver the nanoparticles (NPs) efficiently to the desired location in the context of multiple in vivo physiological barriers. Third, the toxicity of engineered nanomaterials still remains a pendant problem. Fourth, a prerequisite for industrial production and clinical translocation is the cost-effective and scalable fabrication of well-dispersed NPs, which currently still is a great challenge. All these barriers should be overcome for realizing the clinical translocation of the developed nanoformulations. Because of the limitations of the old nano-based formulations, scientists are devoted to searching new nanocarriers with optimized performance. Inorganic nanomaterials have special structures and chemophysical properties. Among inorganic nanomaterials, mesoporous silica nanoparticles have a tailorable mesoporous structure, high specific surface area, and large pore volume. These properties endow them with unique advantages to encapsulate a variety of therapeutic agents and deliver these agents to the desired location. Importantly, the fabrication of MSNs is simple, scalable, cost-effective, and controllable. Being abundantly distributed in nature, silica has

Prof. F. Q. Tang, Dr. L. L. Li
Laboratory of Controllable Preparation
and Application of Nanomaterials
Technical Institute of Physics and Chemistry
Chinese Academy of Sciences
Beijing 100190, P. R. China
E-mail: tangfq@mail.ipc.ac.cn
Dr. D. Chen
Beijing Creative Nanophase Hi-Tech Company, Limited
Beijing 100086, P. R. China

DOI: 10.1002/adma.201104763

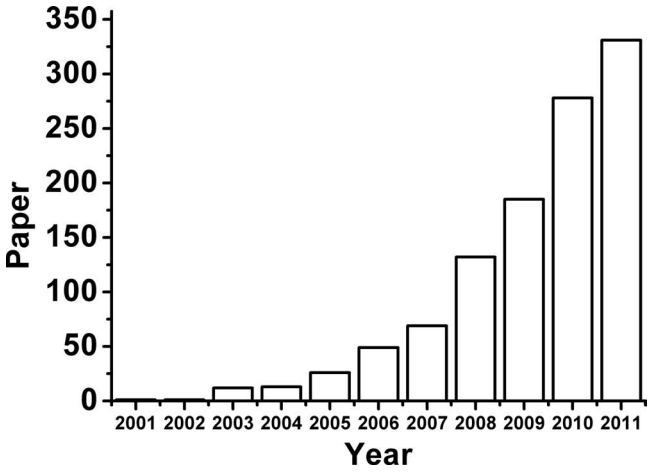

Figure 1. The statistics of the paper indexed in the ISI web of science by the topic of "mesoporous silica" and "drug delivery".

good compatibility and is accepted as "Generally Recognized As Safe" (GRAS) by the FDA and has been widely used in cosmetics and as FDA-approved food additives.[15,16] Thereby, MSNs hold the promise to be developed as versatile drug delivery systems arming toward clinical production. Furthermore, it provides unique opportunities for simultaneous diagnosis and therapy with the MSN-based multifunctional nanocomposites not only as drug delivery system but also as an imaging modality.

To give an overview of recent research progress and future developments of mesoporous silica nanoparticles in biomedical applications, this Review is organized as follows. Firstly, it outlines the controllable synthesis of conventional ordered mesoporous silica nanoparticles and the synthesis strategies of hollow/rattle-type mesoporous silica nanoparticles. It then discusses the biocompatibility of MSNs related to the different physicochemical properties of the nanoparticles. Next, recent progress in drug delivery, especially for cancer therapy, using MSNs and their multifunctional counterparts as drug delivery systems are highlighted. Finally, we conclude our personal perspectives on the directions in which future work on this field might be focused.

2. Synthesis

2.1. Ordered Mesoporous Silica (OMS)

Mesoporous silica nanoparticles with uniform pore size and a long-range ordered pore structure were first reported in the early 1990s using surfactants as structure-directing agents (SDAs).[17,18] Now, rapid progress has been achieved in the synthesis and application of ordered MSNs in catalysis, adsorption, separation, sensing, and drug delivery. With the abundant availability of various types of surfactants and the deep understanding of sol–gel chemistry MSNs with different structures have been developed. The size, morphology, pore size, and pore structure of MSNs can be rationally designed and the synthesis process can be freely controlled. Recently, several reviews have discussed in detail the synthesis of different MSNs.[19–21] In this review, we only emphasize the controlled synthesis of several kinds of MSNs that have been utilized for drug delivery. Until now most research on drug delivery applications of ordered MSNs are based on MCM-41, MCM-48 and SBA-15 type MSNs.

MCM-41 is the most extensively researched type of MSNs for biomedical applications. With the surfactant of cetyltrimethylammonium bromide (CTAB) as liquid crystal templating, tetraethyl orthosilicate (TEOS) or sodium metasilicate (Na_2SiO_3) as the silica precursor, and alkali as catalyst, MSNs with an ordered

Fangqiong Tang is a professor at the Technical Institute of Physics and Chemistry, Chinese Academy of Sciences (TIPC, CAS). She received her B.Sc. degree in chemistry from Beijing Normal University in 1970. She has over thirty years of experience in the preparation and application of nanomaterials. Currently, her scientific interests cover the areas of controlled synthesis of nanomaterials, nanomedicine for cancer diagnosis and therapy, and nano-biosensors for the detection of chemical and biological agents.

Linlin Li is an associate professor at TIPC, CAS. She received her M.Sc. degree in biochemistry and molecular biology from Beijing Normal University in 2005, and Ph.D in chemistry from TIPC in 2008 with Prof. Fangqiong Tang. Her research concentrates on the synthesis and biomedical applications of nanomaterials.

Dong Chen, the General Manager of Beijing Creative Nanophase Hi-Tech Company, has many years of experience with the preparation and application of silica particles and their composites. He received his B.Sc. from Beijing Normal University and his Ph.D from The Hong Kong Polytechnic University with Prof. Yi Li. Currently, he is engaging in commercialization of nanomaterials and nanotechnology.

arrangement of uniform two-dimensional (2D) hexagonal *p6m* mesopores were firstly synthesized and named as MCM-41 (**Figure 2**A).[17,18] In the synthesis, when the concentration is above the critical micelle concentration (CMC), the surfactant of CTAB would self-aggregate into micelles. Around the polar head region of the micelles, the silica precursors condensate at the surface of surfactant and form silica wall around the surface of the micelles. After removal of the surfactant, MCM-41 type MSNs could be obtained (Figure 2B). The specific surface area is high than 700 m^2/g, and the pore size can be tailored in the range of 1.6–10 nm.

For biomedical applications, precise control over particle size, shape, pore size, and pore geometry is very important. Totally, the pore size and its orientation are mainly determined by the nature of surfactant templates. The particle size and morphology can be controlled from sphere-, rod-, to wormlike structures by tailoring the molar ratio of silica precursors and surfactants, pH control using base catalysts,[22,23] addition of co-solvents or organic swelling agents,[24,25] and introduction of organoalkoxysilane precursors during the co-condensation reaction (Figure 2C).[26,27] For instance, we have found that it induces MCM-41 with different specific surface area and pore size using Na_2SiO_3 and TEOS as silica precursors respectively with polyoxyethylene *tert*-octylphenyl ether (Triton X-100) and CTAB as co-surfactants.[28] When Na_2SiO_3 was used as precursor, the synthesized MCM-41 has larger pore and high specific surface area (1379 m^2/g specific surface area and 3.3 nm pore size) than that with TEOS as precursor (848 m^2/g specific surface area and 2.8 nm pore size). This is mainly because the existence of inorganic salt can increase the aggregate number of the surfactant micelles, which further enhances the pore diameters of the MCM-41. We also found that control of the molar ratios of Triton X-100 and CTAB can tailor the morphology of MCM-41.[28] In another research, by simply adjusting the concentration and the molar ratio of CTAB and NaOH, we precisely controlled the aspect ratio (AR) of MCM-41 from spherical to rod-like structure with constant diameter.[29] With the ability to tailor one of the parameters of diameter, aspect ratio, pore size and geometry while keeping other parameters constant, we can research the effect of a certain chemophysical property on biocompatibility and performance in drug delivery of MSNs.

As an important member of the M41S family, MCM-48 also has been paid attention in drug delivery. MCM-48 type MSNs have three-dimensional (3D) bicontinuous structure belonging to the cubic *Ia3d* space group.[30,31] Different from MCM-41 with unidirectional channels, MCM-48 has unique penetrating

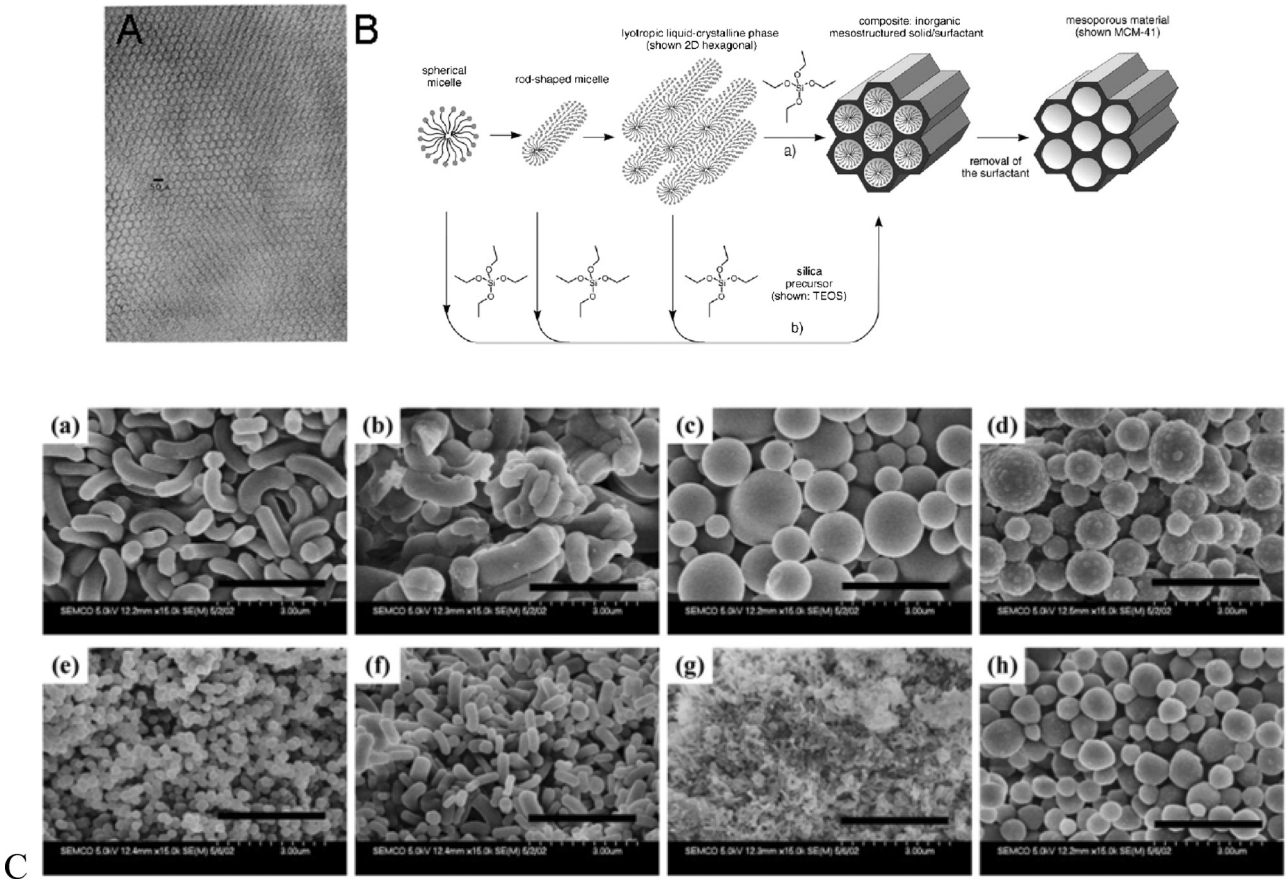

Figure 2. (A) High-resolution transmission electron microscopy (HRTEM) showing MCM-41 with ordered arrangement of uniform mesopores. Reproduced with permission from ref. [18]. Copyright 1992, Nature Publishing Group. (B) Scheme of synthesis of MCM-41 with CTAB surfactant micelles as template. Reproduced with permission from ref. [20]. Copyright 2006, Wiley. (C) Transmission electron microscopy (TEM) of MCM-41 with different size and structure via a co-condensation synthesis method. Reproduced with permission from ref. [26]. Copyright 2003, American Chemical Society.

bicontinuous channels, which are considered to be useful for fast molecular transport and easy molecular accessibility. This property may influence the loading and release of guest molecules for drug delivery. At the early stage of its discovery, the synthesis of MCM-48 is complicated using cationic-anionic surfactants as templates under high temperature and with long reaction time. The synthesized particles are often large than 1 μm and not suitable for drug delivery. Just recently, it has been reported that with a modified Stöber reaction at room temperature using triblock copolymer pluronic F127 as surfactant, monodispersed spherical MCM-48 with particle sizes from 70 to 500 nm can be synthesized.[32] It is important for further biomedical application of MCM-48.

Another widely researched type of MSNs for drug delivery is SBA-15. SBA-15, with 2D hexagonal *p6mm* structure, was firstly synthesized in highly acidic media using amphiphilic triblock copolymer of poly(ethylene oxide)–poly(propylene oxide)–poly(ethylene oxide) ($EO_{20}PO_{70}EO_{20}$, P123) as template in 1998.[33] Generally, it has thicker pore walls and wider pore sizes (5 to 30 nm) than MCM-41.[33] In recent years, sphere and rod-like SBA-15 from micrometer to sub-micrometer range have been synthesized.[34,35] However, it is far away from satisfactory requirements of discretional adjustment of particle size and morphology. Compared with MCM-41, it is still difficult to obtain SBA-15 with small size, especially smaller than 200 nm. Although SBA-15 has adjustable large pore sizes and sturdy silica walls, the large particle size embarrasses their in vivo application. It is believed that if SBA-15 with smaller size could be synthesized, there may have more chance for in vivo application.

In addition, other types of MSNs, such as IBN[36] and FDU-n[37] series mesoporous silica nanoparticles have also great potential in biomedical applications.

2.2. Hollow/Rattle-Type Mesoporous Silica Nanoparticles

With the rapid development of a variety of applications, new demands for mesoporous silica nanoparticles with special structure and performance gradually increase. Recently, hollow and rattle-type nanomaterials have been actively explored for enzyme immobilization, confined-space catalysis, acoustic, thermal and electrical insulation.[38,39] Hollow/rattle-type MSNs with interstitial hollow space and mesoporous shell have low density and high specific area, which are ideal as new-generation drug delivery systems with extraordinarily high loading capacity. For biomedical applications, multifunctionalization or co-delivery of several kinds of drugs are also expected with their special structures. Development of new methods to fabricate hollow/rattle-type MSNs has been one of the hottest topics in nanotechnology.

Conventionally, hollow-type mesoporous silica nanoparticles are fabricated using dual template method with a hard template or soft template to generate hollow interior and a soft template as pore forming agent to induce mesopores in the shell.[40,41] After sol–gel process around the pore template to generate silica matrix coating on the core template, the templates could be removed by thermal calcination or/and solvent extraction. For rattle-type particles, multi-step coating on the core particles is needed to generate a removable middle layer.[42] The fabrication is tedious, high-cost and difficult to fabricate NPs with small size and complicated structure. Now, more and more new methods are under investigation for developing simple, controllable, and scalable fabrication. Various methods such as soft templating, hard templating, layer-by-layer method,[43] Kirkendall effect,[44] Ostwald ripening,[45] and galvanic replacement[46] have been developed for synthesizing a variety of

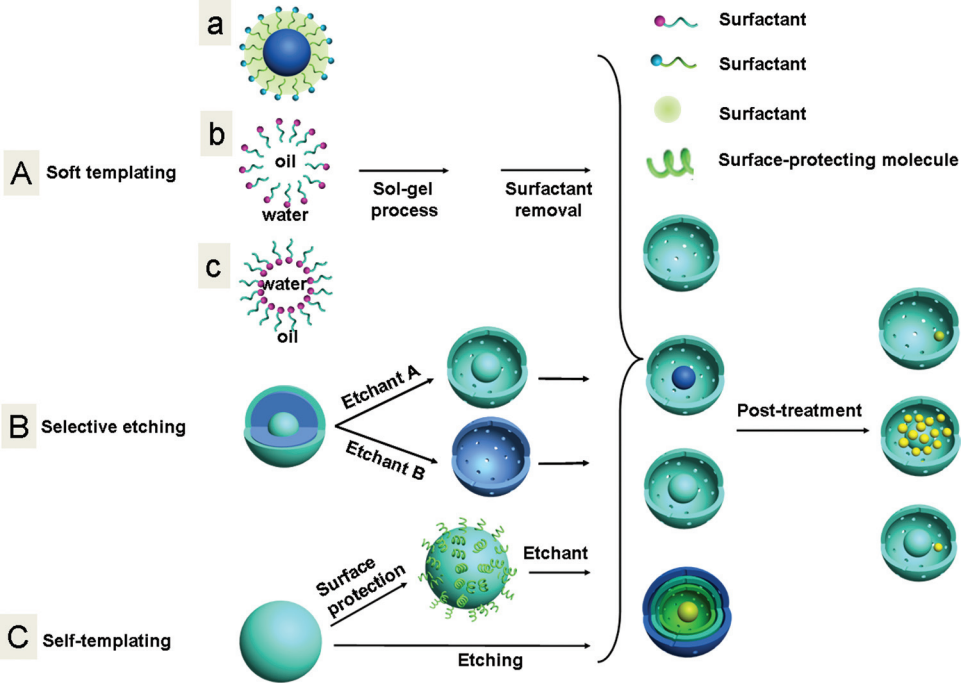

Figure 3. General scheme of methods for the synthesis of hollow/rattle-type mesoporous silica nanoparticles. (A) Soft templating method with a-c) different soft templates, (B) selective etching strategy, and (C) self-templating method.

hollow/rattle-type NPs. Regarding hollow/rattle-type MSNs, herein, we divide the new synthesis methods into soft template method, selective etching strategy and self-template method (**Figure 3**).

2.2.1. Soft-Template Method

Synthesis of hollow/rattle-type MSNs using surfactants as a soft template relies on dual or multi-surfactants to form a complex template for simultaneously building a mesoporous shell and hollow interior (Figure 3Aa). For example, Xu and co-workers dispersed SiO_2 or Au NPs into aqueous mixtures of a zwitterionic surfactant, lauryl sulfonate betaine (LSB), and an anionic surfactant, sodium dodecyl benzenesulfonate (SDBS), to induce the formation of vesicles with movable NP cores.[47] Aminosilane of 3-aminopropyltriethoxysilane (APTES), which acts as a co-structure-directing agent, was then attached to the surfaces of the vesicles. In the following process of sol–gel synthesis, aminosilane can act simultaneously as a vesicle-inducing agent and co-structure directing agent (CSDA). After the surfactants had been removed, the rattle-type silica nanoparticles could be formed. They also fabricated yolk/multishell particles by multiple coating.[48] Similarly, using fluorocarbon surfactant $[C_3F_7O(CFCF_3CF_2O)_2CFCF_3CONH(CH_2)_3N^+(C_2H_5)_2CH_3I^-]$ (FC4) and CTAB as CSDA and 1,2-bis(trimethoxysilyl)ethane (BTME) as hybrid silica precursor, Lu and co-workers synthesized mesoporous organosilica hollow spheres with tunable wall thickness.[49,50] They also used FC4, $(EO)_{106}(PO)_{70}(EO)_{106}$ (F127) and core particles to form a core-vesicle complex as template to fabricate yolk-shell silica particles (**Figure 4**A,B).[51]

Other soft-template methods for generating a hollow interior with assistants of co-template,[52] oil-in-water (O/W) (Figure 3Ab)[53] and water-in-oil (W/O) (Figure 3Ac)[54] microemulsion, water/oil/water (W/O/W) emulsion,[55] and micelle/polymer aggregate[56–61] have also been reported to synthesize porous silica nanomaterials with a hollow or rattle structure. Figure 4C shows the fabrication of porous silica nanoparticles with a W/O microemulsion by Mou and co-workers.[54] They used cyclohexane, Triton X-100, hexanol, and water to form a W/O microemulsion, and aminopropyltrimethoxy silane (APTMS) with TEOS as the silica sources. By adjusting the order and the amount of APTMS addition, they could control the particle size and the interior filling extent. The microemulsion methods are generally preferred for synthesis of sub-100 nm nanoparticles.

Soft template methods are relatively simple and effective for the synthesis of hollow/rattle-type nanomaterials. However, they also have some disadvantages. In general, it is difficult to fabricate nanoparticles with good dispersity and to control the particle size and shell thickness over a broad range. Because a large amount of surfactants is needed in the synthesis process, fabrication of nanoparticles at a large scale is difficult. Another point that deserves mentioning is that it is difficult to remove the template completely while maintaining good dispersity of the nanoparticles. The residual surfactant may result in some undesirable side effects for biomedical applications.

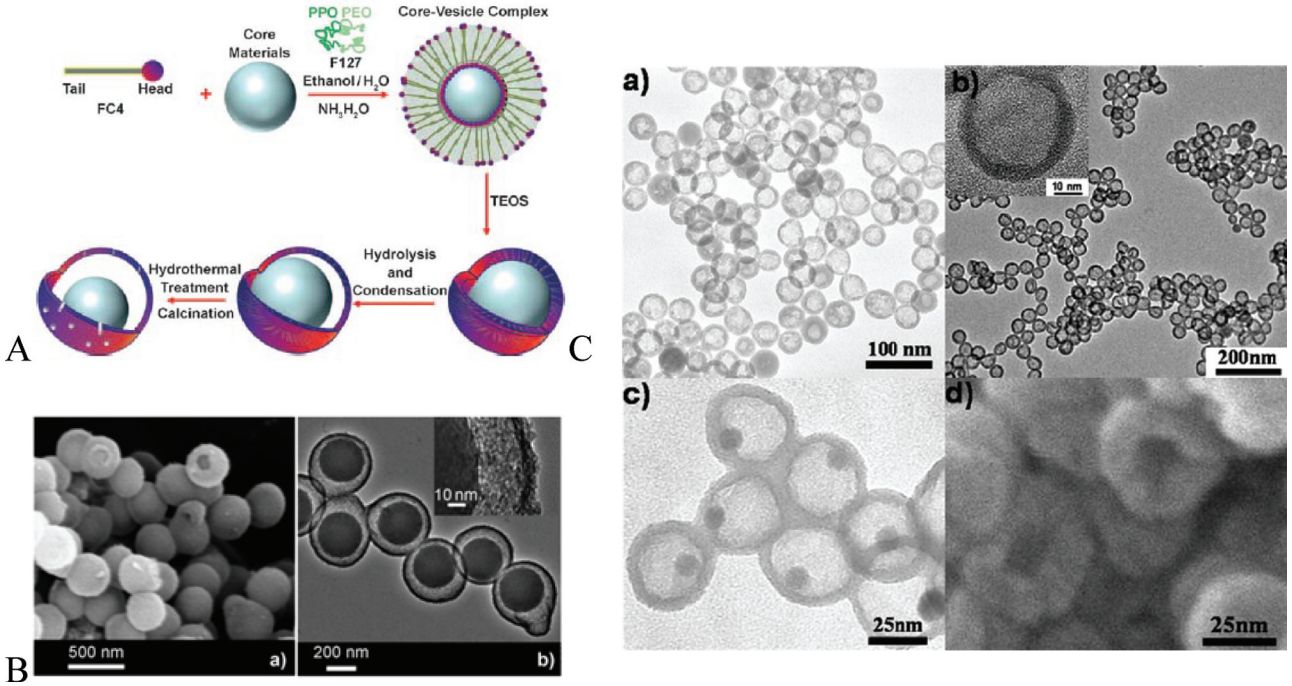

Figure 4. Synthesis of mesoporous silica nanoparticles with hollow/rattle structure via the soft template method. (A) Scheme for preparation of yolk–shell structures with a mesoporous shell using $[C_3F_7O(CFCF_3CF_2O)_2CFCF_3CONH(CH_2)_3N^+(C_2H_5)_2CH_3I^-]$ (FC4) and $(EO)_{106}(PO)_{70}(EO)_{106}$ (F127) as surfactant. (B) a) SEM and b) TEM image of a yolk–shell mesoporous silica nanoparticle synthesized from (A). (A-B) Reproduced with permission from ref. [51]. Copyright 2010, Wiley. (C) Synthesis of hollow silica nanospheres with a microemulsion as template. TEM of a) hollow silica nanospheres, b) dye-modified hollow nanospheres, c) TEM and d) SEM image of dye-modified hollow nanospheres with Fe_3O_4 cores. Reproduced with permission from ref. [54]. Copyright 2009, Royal Society of Chemistry.

2.2.2. Selective Etching Strategy

The so-called selective etching strategy has been developed with the assist of a variety of silylated organic compounds or called organosilane precursors. A pure silica framework and hybrid organic–inorganic networks have different composition and structure, which would induce different stability with different etching agents or under exceptional temperature or pH conditions (Figure 3B).[62] It provides a unique chance for selectively etching the interior layer of a solid nanoparticle to form a hollow structure. In the structure-directed selective etching strategy, the multilayer core/shell solid nanoparticle should be elaborately designed to get hollow or rattle structure.[63,64]

For this purpose, we elaborately fabricated an organic-inorganic hybrid solid silica sphere (HSSS) with a three-layer "sandwich" structure.[65] The core and the outer shell layer of particle were pure silica frameworks hydrolyzed from TEOS, and the middle layer was organic–inorganic hybrid siloxane framework co-condensated from TEOS and *N*-[3-(trimethoxysilyl) propyl]ethylenediamine (TSD). Because the middle layer in which Si–O–Si covalently crosslinks with organic groups hydrolyzed from TSD has less compact structure than the pure silica framework, hydrofluoric acid as etchant has a tendency to selectively etch the middle layer of HSSSs, forming silica yolk/shell structures (silica nanorattle, SN). The selective etching synthesis process is facile, effective, scalable, controllable, and cost-effective. It is convenient to tune the particle size, core diameter and shell thickness in a broad range from sub-100 nm to micrometer length scale (**Figure 5**A). It can synthesize up to 10 g highly monodispersed silica nanorattles in one pot. It provides a sufficient amount of particle samples for researching long-term toxicity and the application in drug delivery. Based

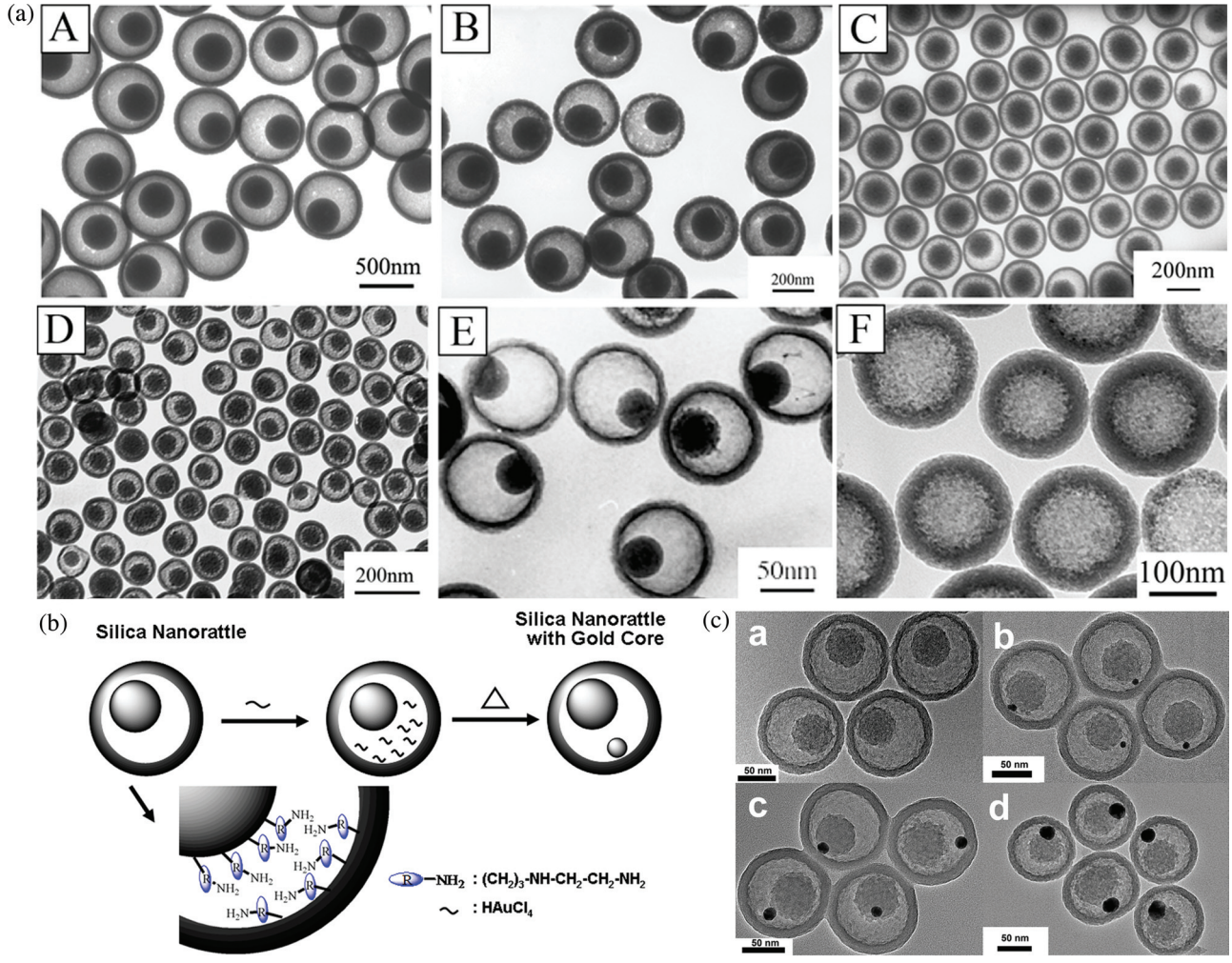

Figure 5. Silica nanorattle with mesoporous and hollow structure synthesized by selective etching strategy. It was used as nanoreactor for synthesis of gold nanoparticle with controllable size in the hollow interior. (A) TEM images of silica nanorattles with different sizes and core/shell ratios: a) 645 nm (core 330 nm, shell 50 nm), b) 330 nm (core 160 nm, shell 40 nm), c) 260 nm (core 140 nm, shell 20 nm), d) 110 nm (core 53 nm, shell 13 nm), e) 95 nm (core 46 nm, shell 15 nm), and f) hollow silica spheres of 170 nm diameter (shell 25 nm). Reproduced with permission from ref. [65]. Copyright 2009, Wiley. (B) Schematic illustration of the preparation of gold core in silica nanorattle with the residual alkylamino groups as reductant. C) TEM images of a) 110 nm silica nanorattle, and silica nanorattle with b) 6.9 nm ± 1.3 nm, c) 15.1 nm ± 2.2 nm and d) 25.4 nm ± 3.9 nm gold core. (B-C) Reproduced with permission from ref. [66]. Copyright 2010, Wiley.

on the slightly modified Stöber reaction, the selective etching strategy guarantees monodispersity of synthesized hollow/rattle-type nanoparticles, as well large-scale fabrication.

With the functional groups in both internal and external surface of silica nanorattles, we have also developed multifunctional silica nanorattles. Using the silica nanorattles as nanoreactors and the residual alkylamino groups as reductant, we synthesized gold nanoparticle with controllable size in the hollow interior of silica nanorattles by a very simple in situ reduction process without any extra reductant (Figure 5B,C).[66] Similarly, without any surface modification, gold nanoshell can be directly coated onto the surface of silica nanorattles with abundant amino groups.[67]

Similarly, Shi and co-workers synthesized solid silica core/mesoporous silica shell nanospheres ($sSiO_2$@$mSiO_2$) with the core hydrolyzed from TEOS and the shell co-condensated from TEOS and octadecyltrimethoxysilane (C_{18}TMS).[68] After treatment of the $sSiO_2$@$mSiO_2$ particles in Na_2CO_3 solution at 80 °C or hydrothermal treatment in ammonia solution, hollow and rattle structure can be formed. They deduced that there exist hydrophobic cores in the particle shell formed by the long carbon chains of C_{18}TMS, which is the pore-making area after burning out the organic carbon chains. The more open structure of the shell facilitates the penetration of the OH^- ions to selectively etch the core part. With this method, they also fabricated rattle-type multifunctional nanoparticles with Fe_2O_3 as core materials and mesoporous silica as shell.[69]

2.2.3. Self-Template Method

Recently, synthesis of hollow mesoporous silica nanoparticles without extra "template" was developed. Here we call it "self-template method" (Figure 3C). In 2005, it was reported that alkaline treatment of cationic polyelectrolyte (poly(dimethyldiallylammonium chloride) (PDDA)) pre-coated mesoporous silica spheres can transfer the nanoparticles to hollow structure.[70] The mechanism was deduced that the hydroxyl ions permeate through the PDDA layer and attack the silica sphere to generate dissolved silicate oligomers under ammonia. The oligomers with negative charge tend to immigrate and deposit onto the positively charged PDDA layer, which then cross-link and finally form a continuous and compact silica-PDDA complex shell. Thereby, PDDA acts as a protector to confine the silica oligomers in the defined room. Similarly, using poly(vinylpyrrolidone) (PVP) as surface protector, Yin and co-workers found that the solid silica sphere can be transferred to rattle-type structure and finally to hollow structure under the treatment of $NaBH_4$ at relatively mild temperature (**Figure 6**A).[71] The mechanism was deduced to be a spontaneous dissolution-regrowth process. They also used NaOH to selectively etch the interior of the silica spheres to form hollow/rattle[72] and multi-shell rattle structures under PVP protection.[73] With surface protectors, these strategies are called "surface-protected etching".

Without any surface protectors, selective etching of the inner space of solid silica nanoparticles to form hollow/rattle structure was also realized.[74–76] Wang and co-workers found the solid silica nanoparticles can transform to hollow/rattle structure after acid treatment under different pH and further hydrothermal treatment at 180 °C.[74] Similarly, Chen and co-workers observed similar phenomenon from solid silica to hollow structure by treating particles at 90 °C for 30 min (Figure 6B).[75] They deduced that the outmost layer of silica nanoparticle by Stöber reaction is "hardest" deriving from the condensation of silicic acid and its aggregates, whereas the innermost layer is "softest" with a porous structure from a lower degree of cross-linking and/or a higher degree of swelling. So the inner layer can be selectively etched by

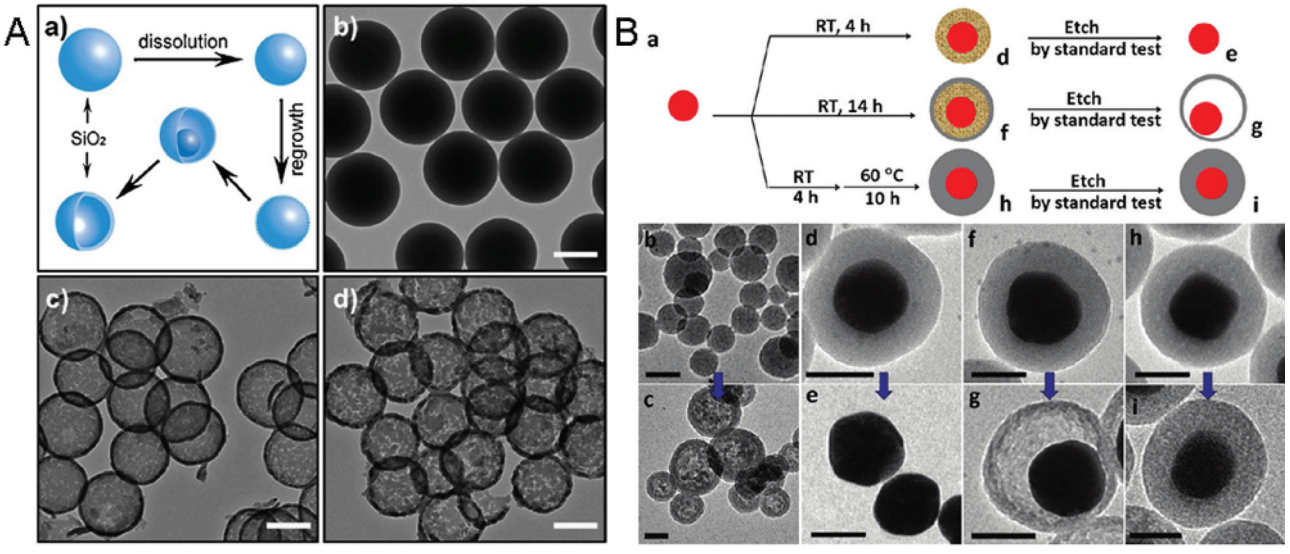

Figure 6. Synthesis of mesoporous silica nanoparticles with hollow/rattle structure by self-template methods. (A) Formation of hollow silica through a spontaneous dissolution-regrowth process. a) Schematic illustration of the spontaneous formation of hollow SiO_2 spheres. b) TEM images of solid SiO_2 spheres. c-d) Hollow silica particles after reacting with different etching condition. Scale bars = 200 nm. Reproduced with permission from ref. [71]. Copyright 2008, Wiley. (B) a) Schematic illustration of selectively etching the inner space of solid silica nanoparticles to form hollow/rattle structure. TEM images showing the experimental conditions and typical nanostructures (b, d, f, h) before and (c, e, g, i) after etching. (b, c) silica NPs, 14 h at room temperature (RT); (d, e) AuNP@silica, 4 h at RT; (f, g) AuNP@silica, 14 h at RT; (h, i) AuNP@silica, 4 h at RT and 10 h at 60 °C. Scale bars = 50 nm. Reproduced with permission from ref. [75]. Copyright 2011, American Chemical Society.

hot water. It is intriguing to get hollow/rattle-type silica nanoparticles from selectively etching Stöber silica particle without any surface protection. As known, Stöber method is the widest used reaction for synthesis of sub-micron silica particles. Previously, silica particles from Stöber method are perceived to be homogeneous in nature. Engineering them with different composition or stability is critically important for selective etching. Now, it has been proven that the Stöber silica particle is inhomogeneous. The new understandings are important for fabricating hollow/rattle type nanostructures with self-template methods.

The advantage of the self-template methods is, the process is simple and the production cost is low. Challenge still exists for scaling up the reaction and synthesizing hollow/rattle-type nanoparticle with good stability and dispersibility.

3. Biocompatibility

Compared to conventional drug nanocarriers, MSNs have a special mesoporous structure and high surface area, which contribute to their various applications in biocatalysis, biosensor, and disease diagnosis and therapy. For in vivo biomedical applications, the particles should fully perform the desired function and avoid non-specific and deleterious changes to the body. Although silica is generally accepted as having low toxicity, the biocompatibility of nano-scaled MSNs as a "new" kind of material should be re-assessed. At a consensus conference of the European Society for Biomaterials in 1986, the word "biocompatibility" was defined as "the ability of a material to perform with an appropriate host response in a specific application". With the rapid development of biomaterials, the scope of "*biocompatibility*" has been widely broadened. Herein, we use *biocompatibility* to include all deleterious and beneficial biological effects caused by MSNs, covering cytotoxicity and in vivo toxicity, and changes of cells and bodies at molecular, cellular, and histological levels. The compatibility of nanoparticles is directly related to their biotranslocation. We also discuss the biotranslocation of nanoparticles themselves in cells and bodies including in vitro cellular uptake kinetics, mechanism, and intracellular trafficking and in vivo biodistribution, metabolism, biodegradation, and excretion. Recently, the chemophysical properties of nanomaterials including particle size, shape, surface area and structure have been proven to play important roles in the particles' biocompatibility and biotranslocation. Establishment of the relationship between these chemophysical properties and the biocompatibility can help us design nanomaterials rationally (**Figure 7**). However, no definite conclusions can be made at this stage about the effects of a certain chemophysical parameter because of the complexity of nanotoxicity research. Some results still are controversial. In this section, we mainly focus on the current data about the effect of size, shape, surface property, and structure on the biocompatibility of MSNs, and try to analyze the possible reasons of the controversial results from different studies.

3.1. Effect of Size

Particle size is considered to be one of the most important properties of nanomaterials. With our increased understanding,

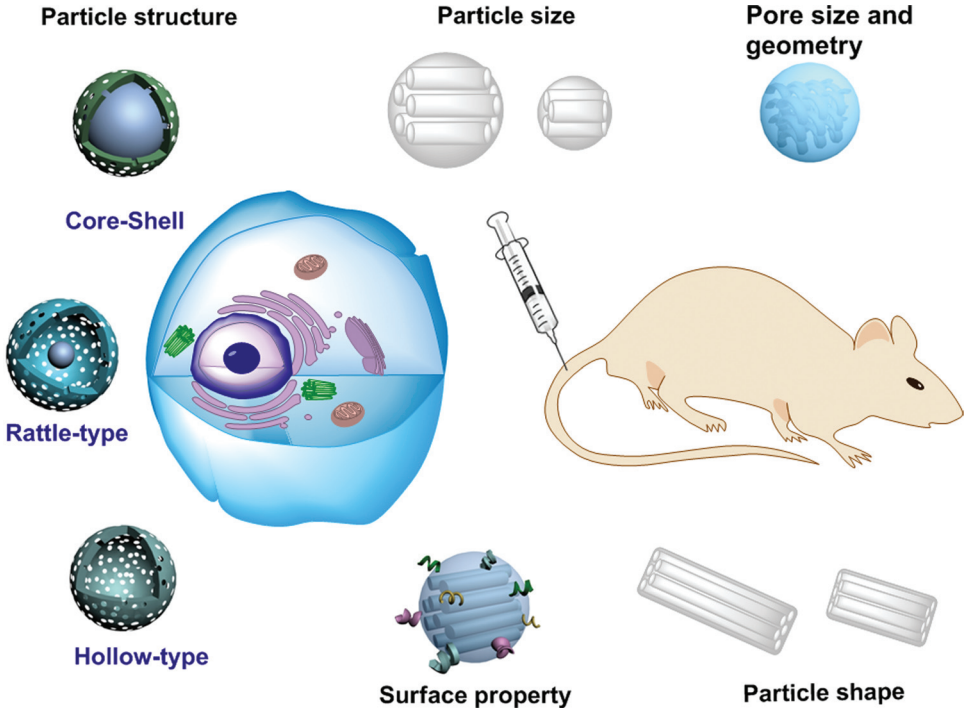

Figure 7. Schematic illustration of biocompatibility and biotranslocation of MSNs. The chemophysical properties of MSNs including particle structure, particle size, pore size and geometry, surface property, and particle shape have a complex influence on in vitro cellular uptake, intracellular translocation and cytotoxicity, and in vivo biodistribution, biodegradation, excretion, and toxicity.

two distinct beliefs have been developed about the size effect on biocompatibility. One belief considers that particle size is one of the most important parameters for the mediation of biocompatibility of nanomaterials, and the other puts forward the opposite conclusion that particle size has an insignificant influence. It is still uncertain what the exact relationship is between particle size and potential toxicological effects of nanomaterials including MSNs.[77]

For the biotranslocation of MSNs, Mou and co-workers investigated the influence of particle size on the cellular uptake of MSNs by Hela cells.[78] The cellular uptake amount is size-dependent in the order 50 nm > 30 nm > 110 nm > 280 nm > 170 nm. The cellular uptake amount of 50-nm nanoparticles was about 2.5 times higher than that of 30-nm particles. This result is consistent with the trend of other nanoparticles that 50-nm particles showed maximum cellular uptake.[79,80] It suggests that 50-nm MSN may be most effective in drug delivery from the aspect of cellular uptake. Another study by Shi and co-workers examined the in vivo biodistribution and urinary excretion of spherical MSNs with a size of 80, 120, 200, and 360 nm by intravenous administration (**Figure 8**).[81] In the research, the particle size is one of the determining factors for in vivo distribution, blood-circulation lifetime and excretion. After intravenous injection, MSNs of all sizes were mainly distributed in the liver and spleen, a minority of them in the lung, and a few in the kidney and heart. The distribution in the liver and spleen increased with the increase of particle sizes from 80, 120, to 200 nm at 30 min post-injection, but the particle with size of 360 nm exhibited different trend of distribution in spleen (Figure 8A,B). Importantly, particles of smaller size had longer blood-circulation lifetime (Figure 8C). The excretion from urine remarkably increased with the increase of particle size, which may reflect the in vivo degradation rates and the excretion amount of degradation products (Figure 8D).

A research on cytotoxicity of spherical MSNs with particle sizes of 190, 420, and 1220 nm found that the cytotoxicity is highly correlated with particle sizes.[82] 190-nm and 420-nm MSNs showed significant cytotoxicity at concentrations above 25 mg/mL, while microscale particles of 1220 nm showed slight cytotoxicity due to decreased endocytosis. Another study found that porous silica particles (25, 42, 93, 155, and 225 nm) caused a concentration- and size-dependent hemolytic activity.[83] The smaller particles have higher hemolytic activity than the larger ones. However, these in vitro results have not been validated by in vivo studies. It has been found that MSNs with sizes of 150 nm, 800 nm, and 4 μm showed a size-independent toxicity in vivo instead with a significant dependence on route of administration.[84] When intraperitoneal and intravenous injection of

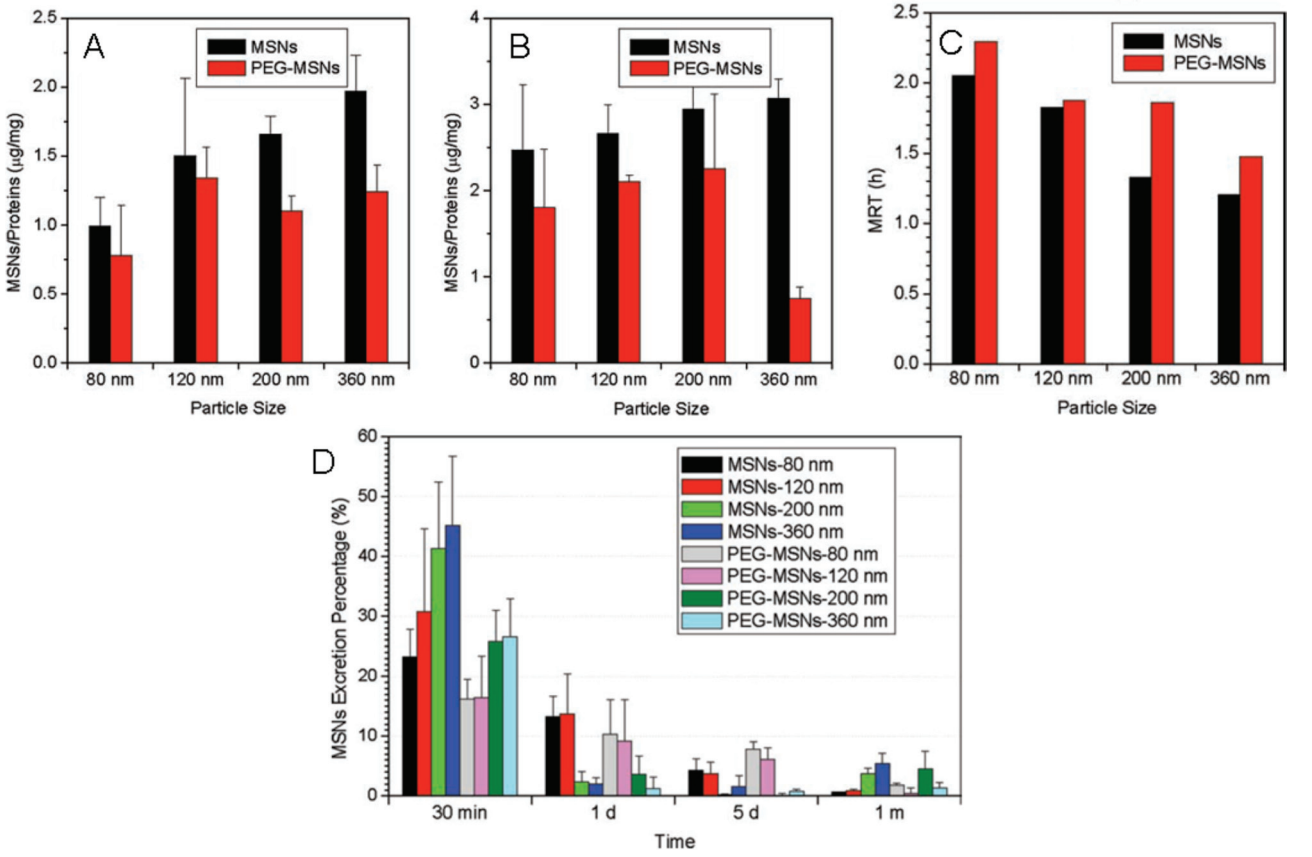

Figure 8. ICP analysis of in vivo biodistribution and urinary excretion of MSNs with effect of of particle size and PEGylation. Biodistribution of MSNs and PEG–MSNs of different particle sizes (80, 120, 200, and 360 nm) in (A) liver and (B) spleen of ICR mice at 30 min after intravenous injection. (C) Size-dependent mean residence time of MSNs and PEG–MSNs in blood of Sprague–Dawley rats. (D) Excretion of MSNs and PEG–MSNs in urine of mice after intravenous injection. Reproduced with permission from ref. [81]. Copyright 2010, Wiley.

1200 mg/kg MSNs in mice resulted in death, no obvious toxicity was observed with subcutaneous administration of the same particles in the same dose. Our recent studies on the single and repeated toxicity in mice of silica nanorattles (SNs) with sizes of 70, 110, and 260 nm found that the single dose toxicity exhibits a size-dependent relationship. However, the effect of size on subacute toxicity is insignificant instead with a dose-dependent hepatotoxicity (unpublished data). The underlying mechanism that results in differential single and repeated toxicity related to particle size is still being investigated.

3.2. Effect of Surface Properties

Besides size, the surface properties are considered to be the most important aspect that influences the biocompatibility of nanoparticles. Different from other chemophysical parameters, the effects of surface properties have received recognition from the scientific community. It is commonly accepted that nanoparticles with a cationic charge would induce more immune response and cytotoxicity than the neutral and anion counterparts but are advantageous for transvascular transport in tumors, whereas particles with a neutral charge show favorablly long circulation times and interstitial transport in tumors.[85,86]

Although it is estimated that the surface silanol groups exposed toward the external environment is only less than 6% of the total of the particles, the exposed silanol group can interact with biological molecules, such as cellular membrane lipids and proteins, and destroy the structure of these molecules.[87] Without surface modification, the bared MSNs with negative zeta potential would rapidly associate with serum opsonin, and then be cleared from circulation by macrophages in reticuloendothelial system (RES) after entering into the blood stream. Surface modification of MSNs plays pivotal role in altering the surface reactivity, improving the biocompatibility and increasing in vivo circulation time.

The most efficient surface modification strategy is PEGylation. Polyethylene glycols (PEGs), approved by FDA, can form a hydrophilic layer around particles with increased dispersity, and can greatly increase the half-life by delaying opsononization.[88] It acts as a protecting layer to mask the reactive surface silanol groups and prevent the access of additional silanol groups from collapsed pores.[83] It was reported that mesoporous nanoparticles after PEGylation have decreased distribution in RES related tissue of liver and spleen after intravenous administration. Meanwhile, the blood-circulation lifetime is prolonged and excretion rate is decreased.[81,89] PEGylation also can ameliorate the hemolytic activity and cytotoxicity, and decrease the endocytosis of mesoporous silica nanoparticles.[90,91]

Nevertheless, PEGylation is not the gold standard for escape of RES. It has some limitations.[92] Although the common belief is that PEGylation can prevent immune recognition, recent studies have suggested that the PEGylated nanoparticles would induce production of specific anti-PEG IgM that is responsible for accelerated blood clearance (ABC) of nanoparticles after repeated injection.[93] It also results in hypersensitivity reaction by complement cascade activation in blood.[94]

Other surface modifications of MSNs have also been researched. Because of existence of abundant silanol groups, modification of the particles surface is relatively facile. It has been suggested that the in vitro cellular uptake and cytotoxicity,[95–98] and the in vivo biodistribution and excretion[99] of MSNs can be regulated by different surface functionalization via amino (-NH_2), carboxyl (-COOH), phenyl (-Ph), and methyl phosphonate (-PO_3^-) groups with negative, neutral, and positive zeta potentials. In one example, surface-modification of MSNs (fluorescein isothiocyanate (FITC) functionalized) with functional groups, 3-amino-propyl (AP), guanidinopropyl (GP), N-(2-aminoethyl)-3-aminopropyl (AEAP), and N-folate-3-aminopropyl (FAP) could manipulate the particle endocytosis by Hela cells (**Figure 9**A).[95] The plots of the logarithms of the concentrations of MSNs versus the percentages of cells that took up the MSNs showed a sigmoidal behavior with dose-response endocytosis (Figure 9B). MSNs with different surface modification were endocytosed by Hela cells via different endocytosis pathway: FITC- and FAP- MSNs were endocytosed via clathrin-pitted mechanism, FAP-MSNs were endocytosed by folic acid receptors, and AP- and GP-MSNs were endocytosed via caveolae-mediated mechanism (Figure 9C).

Coating MSNs with lipid layer was utilized to improve the biocompatibility and performance.[100–104] PEG-LipoMSNs, assembled from PEG-derived phospholipids on the particle surface of 200 nm MSNs, exhibited superior suspensibility and much lower nonspecific binding in vitro compared to the bare MSNs.[101] In another study, 34.3 nm silica nanoparticles coated with lipid have increased bioapplicability with more than 10 times prolonged half-lives, and decreased distribution in RES-related organ.[102]

3.3. Effect of Shape

In the past several years, particle shape has gained more and more attention[105–108] since it was found that nonspherical particles have reduced phagocytosis by macrophages and longer in vivo circulation time.[106,109] However, it is difficult to take shape as a single variable and establish the relationship between particle shape and biocompatibility because fabrication techniques to produce particles with different shapes using biocompatible materials are limited.[110] The possibility of fabricating MSNs with different shape and similar composition, structure, diameter, and dispersity enables us to research the shape effect on nanotoxicity, biodistribution, and performance for drug delivery.

About the effect of particle shape on cellular endocytosis, a theoretical model was proposed in 2005 to compare the cell membranes containing diffusive mobile receptors that wrap around a ligand-coated cylindrical or spherical particle.[111] In this model, the concept of "wrapping time" was introduced to explain the faster endocytosis of spherical particles than the cylindrical ones. Another simulation deduced that the shape anisotropy and initial orientation of particles are crucial for the interaction between the particles and the lipid bilayer of cellular membrane using dissipative particle dynamics (DPD).[112] To some extent, these models provide useful guidance for shape consideration in designing drug delivery systems. However, what is not included in these theoretical models is the cell-type specific variation, which would result in different endocytosis

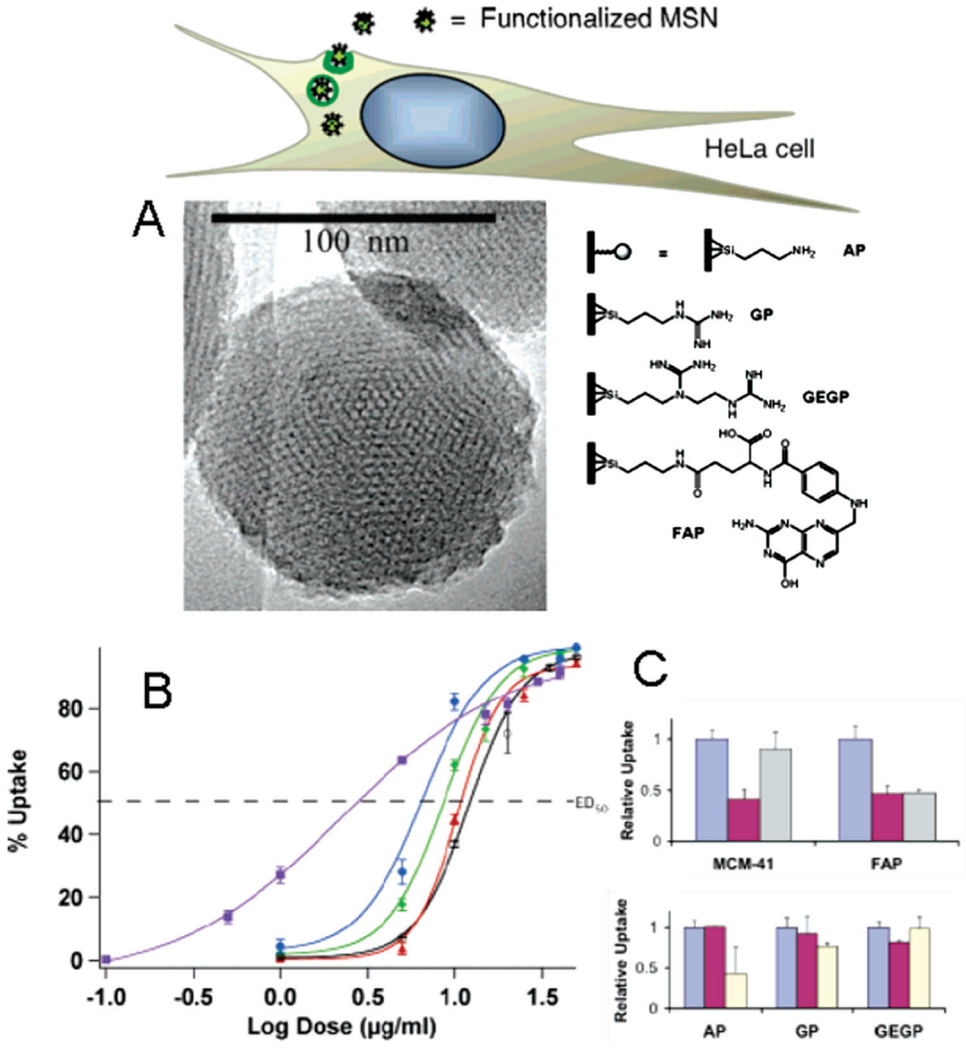

Figure 9. Effect of surface functionalization of MSNs on endocytosis by Hela cells. (A) Schematic representation of the endocytosis of organically functionalized MSNs with 3-amino- propyl (AP), guanidinopropyl (GP), N-(2-aminoethyl)-3-aminopropyl (AEAP), and N-folate- 3-aminopropyl (FAP). (B) Uptake of the synthesized MSNs as a function of their concentration: (○) FITC-, (▲) AP-, (□) GP-, (●) GEGP-, and (■) FAP-MSNs. (C) Uptake of the materials in absence (blue bars) and presence of a series of inhibitors: 450 mM sucrose (prune); 1 mM folic acid (gray); 200 mM genistein (cream). Reproduced with permission from ref. [95]. Copyright 2006, American Chemical Society.

pathway of nanoparticles due to differential receptor expression among various cell lines, and further determine the different endocytotic rate, intracellular trafficking and final fate. Thus, it is explicable that the experimental results sometimes are not consistent with that from theoretical models.

Until now, research on the shape effect of MSNs have mainly focused on in vitro cellular uptake. As reported, cellular uptake of spherical (size distribution from 80 to 150 nm) and tube-shaped (600 nm in length and 100 nm in width) MSNs by Chinese hamster ovarian (CHO) cells and human fibroblast cells was both morphology- and cell line-dependent.[113] For CHO cells, the endocytosis rates for both MSNs were similar and rapid, whereas endocytotic rate of sphere MSNs was significantly faster than that of rod-like MSNs by fibroblast cells. However, the two kinds of particles in high concentration were aggregated, which would definitely influence the final readout of the shape effect. Another study used MCM-41 (500–900 nm with spherical or oval shape) and SBA-15 (irregularly shaped and micrometer sized) type MSNs for delivery of platinum drugs.[114] The uptake of MCM-41 and SBA-15 by Jurkat cells (leukemia cell) was via phagocytosis and receptor-mediated endocytotic pathway, respectively. Recently, Nel and co-workers compared the cellular uptake of different shaped MSNs including MSNP0 (AR = 1~1.2), MSNP1 (AR = 1.5~1.7), MSNP2 (AR = 2.1~2.5), and MSNP3 (AR = 4~4.5). MSNP2 with an AR of 2.1–2.5 were taken up by Hela cells via small GTPase-dependent macropinocytosis with larger quantities over the shorter or longer length rods, which subsequently induced more efficient drug delivery of paclitaxel.[115] Another study by Ghandehari and co-workers on the cytotoxicity of MSNs with diameter of 80~150 nm and aspect ratio of 1, 2, 4, and 8 showed that aspect ratio had no significant effect on the particles' acute cytotoxicity, proliferation inhibition, plasma membrane integrity, and cellular uptake to murine macrophage, human lung carcinoma cells and human

erythrocytes.[116] However, the hemolytic activity was shape-dependent MSNs with higher aspect ratio showed lower hemolytic toxicity. The different cellular uptake behavior of MSNs with similar aspect ratios in these respective studies is likely due to the difference in other parameters including diameter of MSNs, selection of cell line, and existence of serum protein in the research systems.

With controllable synthesis of MSNs and fluorescent counterparts with aspect ratios from 1 to 10 (**Figure 10**A), we investigated the interaction between A375 human melanoma cells and MSNs with dimmer of about 100 nm and aspect ratio of 1, 2, and 4.[107] Overall, particles had a greater impact on different aspects of cellular functions including cell proliferation, apoptosis, cytoskeleton formation, adhesion and migration with the increase of the aspect ratio (Figure 10B), which may result from the accelerated cellular internalization rate and increased uptake amount (Figure 10C). In addition to cellular behavior, we also examined the protein expression related to cell adhesion, cell adhesion molecule-1 (ICAM-1) and melanoma cell adhesion molecule (MCAM) at protein and mRNA expression level.[107] The influence of protein expression by the aspect ratio of a particle followed the same trend as the cellular behavior. Our recent research on cellular uptake mechanism of differently shaped MSN found that spherical particles preferred to be internalized via a clathrin-mediated pathway in Hela cells while MSN with large ARs favored to be internalized via caveolae-mediated pathway (Unpublished Data). The different cellular uptake pathways would finally determine the intracellular fate of the nanoparticles as drug delivery systems.

Up to now, little attention has been paid to in vivo behavior of MSNs related to shape. We recently found that the in vivo biodistribution, clearance, and biocompatibility of MSNs and PEGylated counterparts with aspect ratios of 1.5 and 5 and diameters of 110~150 nm were dependent on the shape and surface modification.[29] At 2 h post-intravenous injection, short-rod MSNs (NSR) were easily trapped in the liver, while more amount of long-rod MSN (NLR) distributed in the spleen (Figure 10D). PEGylation can decrease the RES sequestration by the liver and spleen for both shaped MSNs. In terms of the circulation time of particles in blood, the NLR and NSR did not show detectable concentration differences in blood at 2 h after administration. At 24 h, the Si content of NSR in blood significantly deceased, whereas that of NLR maintained at a similar level as that of 2 h, indicating that NLR has a longer blood circulation time than NSR, consistent with previous reports for other materials.[106,117] We also found that short-rod MSNs had a more rapid clearance from urine and feces than long-rod MSNs in both excretion routes (Figure 10E). All these findings may

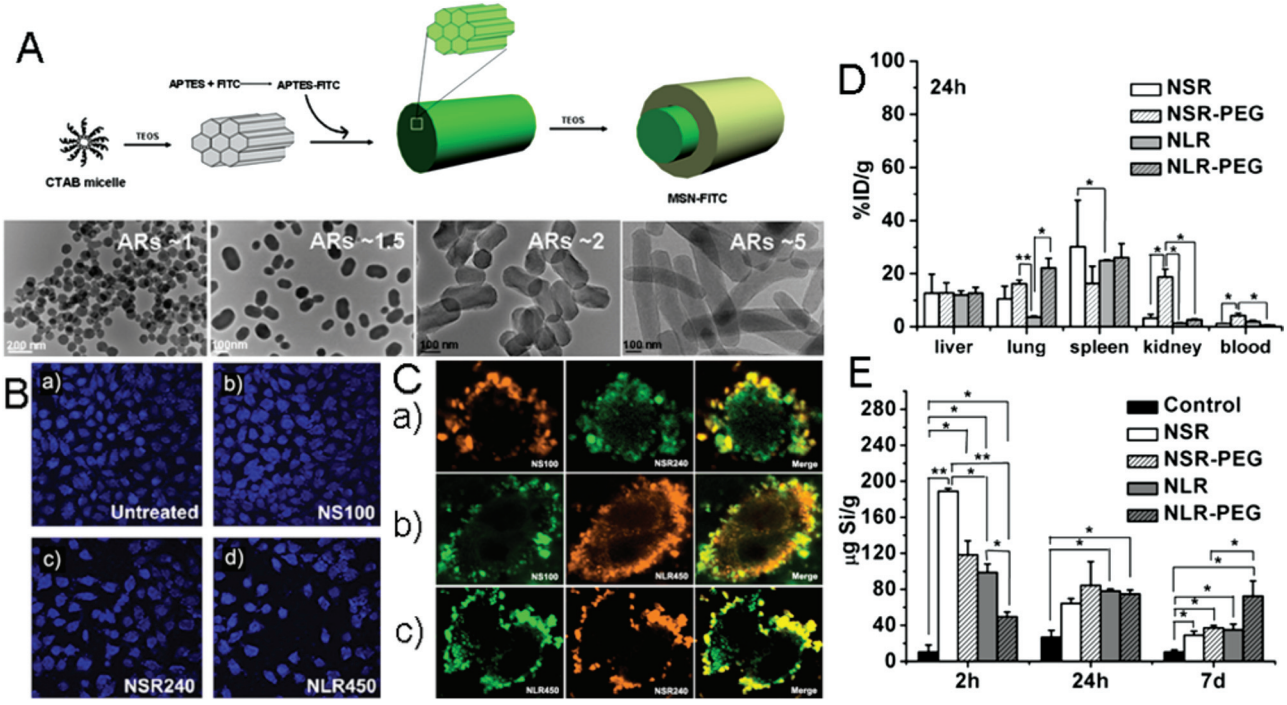

Figure 10. Controlled fabrication of MSNs with different aspect ratios and their effect on the in vitro and in vivo behaviors. (A) Illustration of the fabrication of MSN-FITC with aspect ratio from 1 to 5 and the TEM images of nanoparticles.[29] (B) A375 cellular adhesion was influenced by nanoparticle with different aspect ratios. a) Negative control, b) sphere MSN, c) short-rod MSN (aspect ratio = 2), and d) long-rod MSN (aspect ratio = 4).[107] Copyright 2010, Elsevier. (C) A375 cellular uptake simultaneously incubated with two kinds of MSN labeled with different fluorescence. a) Sphere MSN (RITC-labeled, red), short-rod MSN (aspect ratio = 2; FITC-labeled, green), and merge fluorescent image; b) sphere MSN (FITC, green), long-rod MSN (aspect ratio = 4; RITC-labeled, red) and merge fluorescent image; c) long-rod MSN (aspect ratio = 4; FITC-labeled, green), short-rod MSN (aspect ratio = 2; RITC-labeled, red) and merge fluorescent image. FITC: fluorescein isothiocyanate; RITC: rhodamine B isothiocyanate. Reproduced with permission from ref. [107]. Copyright 2010, Elsevier. (D) Relative silica contents in liver, spleen and kidney at 24 h post intravenous injection of short-rod MSN (aspect ratio = 1.5) and long-rod MSN (aspect ratio = 5). Reproduced with permission from ref. [29]. Copyright 2011, American Chemical Society. (E) Si content in urine at 24 h post intravenous injection of short-rod MSN (aspect ratio = 1.5) and long-rod MSN (aspect ratio = 5). Reproduced with permission from ref. [29]. Copyright 2011, American Chemical Society.

provide useful information for the rational design of efficient drug delivery nanocarriers and therapeutic systems and provide insights into nanotoxicity.

To confirm the influence of shape of MSNs more precisely, more rigorous research is needed. Currently, evidence clearly shows that the shape does have an important influence on the cell–nanoparticle interaction and in vivo particle biotranslocation. In a recent study,[118] it was found that a rod of 15 nm diameter and 54 nm length (CdSe/CdS quantum dot (QD) coated with silica shell) penetrated tumors 4.1 times faster than 35-nm diameter spheres (CdSe QD). This result reminds us that MSNs with large aspect ratio and suitable diameter may have longer circulation time and more efficient tumor accumulation than the spherical ones, which may significant enhance the therapeutic efficacy of nanoparticulate drug delivery systems.[119]

3.4. Effect of Structure

In recent years, the development of MSNs with novel structures has attracted great interest for biomedical applications. Structure as one of the greatest contributors to the properties of MSNs has been given little attention with respect to biocompatibility. Would the pore size and geometry, surface area, existence of the void space of hollow structure, matrix with or without porosity influence the biocompatibility and biotranslocation of MSNs? It remains to be answered. Because of the diversity of engineered MSNs, it is rather difficult to extract a certain chemophysical parameter independently for accurately discerning its influence.

Sharing the same composition with non-porous colloidal silica, MSNs have porous structure, low density, and large surface area. The high specific surface area may be advantageous for encapsulating guest molecules, but meanwhile may pose an increased risk and hazards with higher reactive and oxidative activity.[120] It has been generally accepted that the specific surface area is positively correlated with the toxicity of nanoparticles. Nanoparticles with large surface areas and abundant silanol groups have the ability to generate reactive oxygen species (ROS), which play significant role in nanomaterial-caused injury.[120] It has been demonstrated that MSNs can inhibit cellular and mitochondrial respiration[121] and cause oxidative stress.[122] However, comparison of the toxicity of porous and non-porous silica nanoparticles results in opposite experimental results. Recently, it was found that spherical MSNs with a diameter of 100 nm showed less cytotoxicity, inflammatory response, and contact hypersensitivity than the colloidal solid counterparts (**Figure 11**).[123] Similarly, two other studies found MSNs had lower hemolytic activity[83] and cytotoxicity[124] than the nonporous counterparts. The reason is deduced as follows: the "cell-contactable surface area" of nanoparticles decides the nanoparticle-organism interaction. Although the surface area is higher for porous silica than the nonporous counterpart, the "cell-contactable surface area" that the area with which cell membrane, cell-bound proteins, and cell-associated molecules can interact, is less for porous silica nanoparticles instead.

An important point that deserves to be mentioned is the influence of structure on biodegradation. The possible toxicity risk caused by inorganic nanomaterials has greatly retarded the translation of preclinical research into clinical trials. It has been demonstrated that the intracellular lysosomal environment is not sufficient for biodegradation of silica nanoparticles. Could MSNs be degraded into excretable nontoxic monomers and finally be excreted from body? It has been found that surfactant-extracted MSNs have a remarkably faster degradation rate in simulated body fluid than the calcined MSNs and the amorphous solid silica.[125] As mentioned above, the in vivo degradation rate of MSNs is also influenced by particle size and surface modification.[9,81] The biodegradability of MSNs with a controllable degradation rate makes it suitable for biomedical applications.

Mesoporous particles with a hollow structure have huge voids to accommodate therapeutic agents. However, we currently have little understanding about the effect of hollow structure on the biocompatibility and particle biotranslocation. Would the low density and hollow structure influence the in vivo dispersity, biodegradation, flow and adhesion in blood vessels, and subsequently control the distribution, clearance, and passive tumor accumulation of MSNs?[126] We studied the in vivo toxicity and biodistribution of silica nanorattles with mesoporous and hollow structure. The lethal dose 50 (LD_{50}) of 110 nm SNs was higher than 1000 mg/kg.[127] No death was observed when mice were exposed to SNs at 20, 40, and 80 mg/kg by continuous intravenous administration for 14 days. After intravenous administration, the silica nanorattles would be captured by the mononuclear phagocytic cells in liver and spleen. The particles can be excreted from mice with an entire clearance time over 4 weeks. These results suggest low toxicity of silica nanorattles when intravenous injection at single dose and repeated administrations. Notwithstanding the undetermined influence of hollow structure on the interaction of nanoparticles with body, it provides necessary prerequisites for further development of the silica nanorattle as effective drug delivery system.

Summarily, MSNs should no longer be considered as simple drug carriers for biomedical applications. They can also play an active role in mediating biological effects. The chemophysical properties of MSNs including particle size, surface properties, shape and structure and so on have been proven to have remarkable influence on the biocompatibility of MSNs. The inconsistent results of separate studies may attribute to several reasons. First, it is important to fix the physicochemical parameters other than the object parameter to make a valid conclusion. In some studies, it was not fully considered. Second, the nanoparticles after entering into body may be aggregated by absorption of blood serum protein. Removal of the surfactant template by thermal calcination or solvent extraction also may result in agglomeration of the nanoparticles. Thus, the primary particle size and shape may no longer be effective parameters in tuning the biocompatibility of nanoparticle. Third, the range of particle size, shape, and dose selected for evaluation may be not overlapped in different studies. There may be different trends of biodistribution and toxicity in different ranges. Fourth, the in vivo biotranslocation process of nanoparticles is so complicated that the current evaluation level and methodology are still limited to thoroughly detecting all the changes caused by nanomaterials. With the explosive increase in research on biomedical

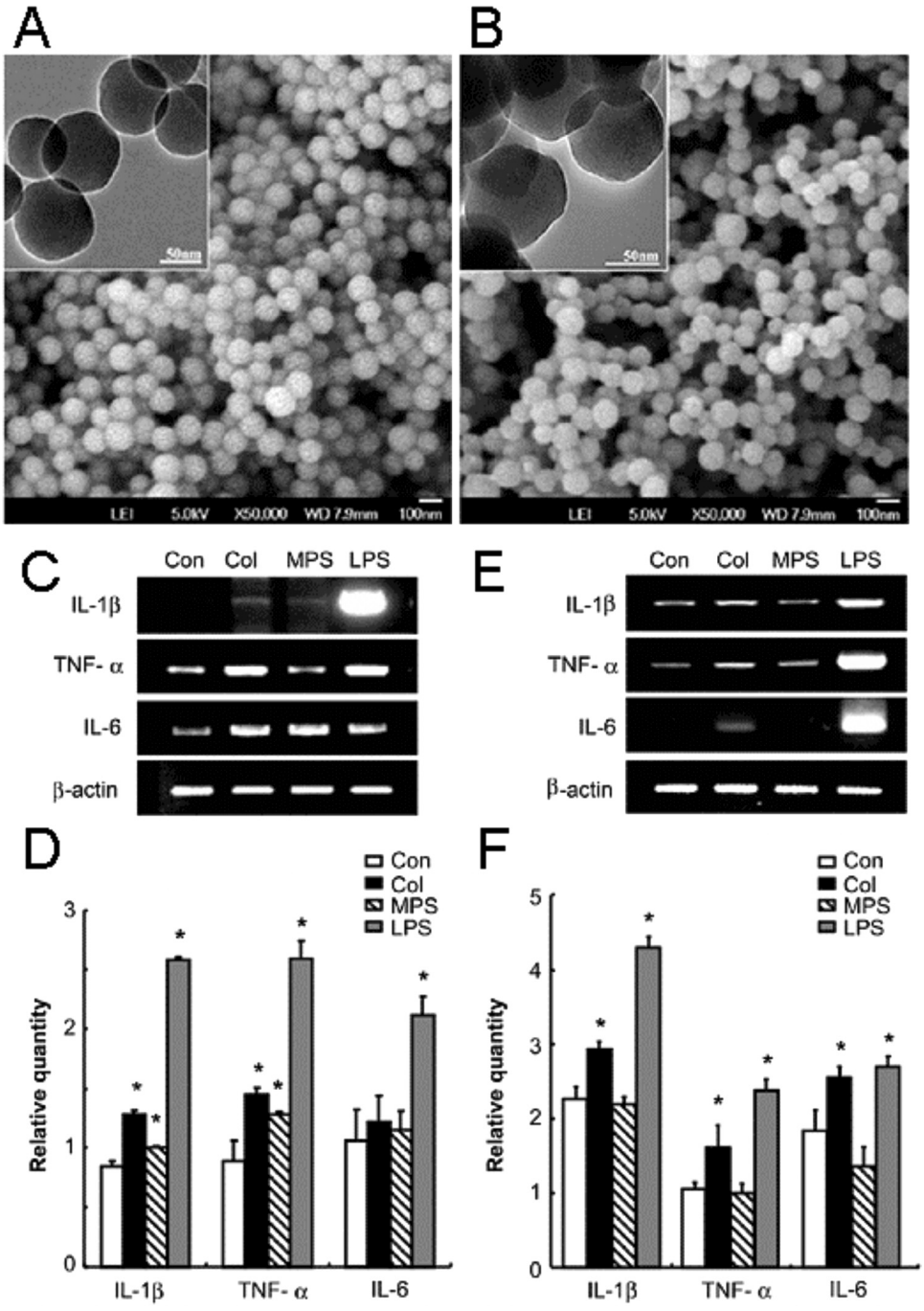

Figure 11. SEM and TEM of (A) colloidal silica, and (B) mesoporous silica nanoparticle. Effects of nanomaterials on expression of pro-inflammatory cytokines. mRNA level of TNF-a, IL-1b, and IL-6 cytokines by RT-PCR and real-time PCR in (C-D) J774A.1 cells or in (E-F) primary peritoneal macrophages. Col: colloidal silica nanoparticles; MPS: mesoporous silica nanoparticles; LPS: lipopolysaccharide used as positive control. Reproduced with permission from ref. [123]. Copyright 2011, Elsevier.

applications, more attention needs to be paid to the biocompatibility of MSNs concurrently. Establishment of the nanoparticles–organism relationship is needed for choosing nanocarriers with low or without toxicity. Otherwise, new methodologies such as computational nanotoxicology[128] and high throughput screening[77] are expected to help us select and design safer and more effective MSNs.

4. Drug Delivery

4.1. MSN-Based Drug Delivery System

In 2001, Vallet-Regí firstly reported the application of MSNs as a drug delivery system.[1] They loaded ibuprofen, an anti-inflammatory drug, into the mesopores of MCM-41 type MSNs,

which exhibited high drug loading capacity and sustained drug release. With the gradually increased research, MSNs have been proved to be advantageous in loading a wide range of therapeutic agents including pharmaceutical drugs, therapeutic proteins, and genes. They are more flexible, versatile, and robust than conventional drug delivery systems such as polymer nanoparticles, liposomes, and so on. The limitations of conventional organic nanocarriers are considered to be heterogeneous distribution of drug through the matrix, low drug loading capacity, low yield and high-cost of production. With the special mesoporous structure and high specific surface area, MSNs as reservoirs have a high capacity to accommodate guest molecules, and can release the loaded molecules in physiological conditions. Their long-range ordered pore structure with tailorable pore size and geometry facilitates a homogenous incorporation of guest molecules with different sizes and properties. Another important advantage of MSNs is the well monodispersity and dispersity, and tailored size and structure, ensuring coincident and controllable in vivo pharmacokinetics and predictable outcome. Furthermore, large-scale production ability is an easy to be ignored advantage of MSNs over the polymer and liposomal drug carriers in pharmaceutics. The manufacture process is relatively simple and the cost is significantly low, which is very important to fulfill the future clinical demand and the commercialization.

4.1.1. Effect of Chemophysical Property on Drug Delivery

The essential function of drug delivery systems includes their ability to increase drug solubility, and change the drug metabolism and pharmacokinetics (DMPK) for increasing the drug accumulation in targeting location and decreasing the off-target distribution and unwanted toxicities. The drug loading capacity and drug release profile are the most important performance indicators of a drug delivery system.

MSNs have an open entrance for drugs to enter in, and well-ordered channels for homogeneous distribution of drug molecules. Drug loading and release are very different to that from a polymer matrix.[129] The pore diameter,[1] pore topology and helicity,[130,131] surface properties,[132] and so on would significantly influence the drug loading capacity, the host-guest interaction, and the final drug release behavior. Thus, for a given drug molecule, MSNs should be carefully designed and corporately tailored for desired drug loading and release properties. The pore diameter of MSNs is considered as size-selective adsorption parameter of drugs. Drug molecules larger than the pores of MSNs could not be effectively absorbed into the mesopores. Thus, biomacromolecules with large molecular weight and large-volume such as proteins and genes correspondingly need large pores for commendation.[133,134] For instance, Vallet-Regí and co-workers found that the pore size of MCM-41 can control the amount of absorbed ibuprofen and the drug releasing kinetics due to different packing geometry of drug molecules in the pore of different size.[135] The surface property is another important factor.[136,137] The host-guest interaction is mainly a chemical interaction between free silanol groups and functional groups of the guest molecules. For controlling the interaction with guest molecules, MSNs can be modified with different functional groups at the surface and the mesopore walls, resulting in a different surface potential, functional groups, and hydrophobic/hydrophilic property of the matrix surface. Vallet-Regí and co-workers reported that modification of MSNs with quaternary organic amines of different alkyl lengths could increase the loading capacity of L-tryptophan (L-Trp), a hydrophobic model amino acid, for more than 10 times.[132] Shi and co-workers grafted high-density carboxyl groups onto the pore surface of MSNs, which served to complex with platinum atoms, leading to much increased drug loading efficiency of cisplatin.[138] Indeed, tuning the host-guest interaction is essential for both drug loading and release. Researches on the interaction mechanism between the nanomaterials and guest molecules is extraordinarily important. Recently, using single-molecule fluorescence microscopy, Brauchle and co-workers directly observed the diffusion of single molecule of doxorubicin (DOX) inside the mesoporous silica with different pore size and structure.[130] It was shown that pore diameter control and pore functionalization offered possibilities to fine-tune host-guest interactions and control the dynamics of drug release.

4.1.2. Drug, Protein and Gene Delivery

With the versatile and tunable structures, MSNs have been proven to be capable of loading a variety of guest molecules including pharmaceutical drugs, therapeutic peptides and proteins and genes. MSNs have been used as drug delivery systems of kinds of pharmaceutical drugs of different hydrophobic/hydrophilic properties, molecule weights, and biomedical effects such as ibuprofen,[1] doxorubicin,[139] camptothecin,[140] cisplatin,[138] and alendronate arming at their essential requirements (**Figure 12**).[141] For example, the main obstacle of a lot of oral drugs is their poor intestinal adsorption with poor bioavailability. Augustijns and co-workers used MSNs as drug carrier of poor water-soluble oral drug of itaconazole for a significantly enhanced oral bioavailability with AUC_{0-24} of 1069 ± 278 nM h compared with free drug (the marketed formulation of Sporanox) with a AUC_{0-24} of 521 ± 159 nM h in rabbits.[142]

Peptide and protein drugs have been developed as potent therapeutic agents in many medical applications including cancer therapy, vaccination, and regenerative medicine. However, due to their intrinsic properties of large molecular weight and fragile structure, protein delivery is rather difficult.[143,144] Attributed to the porous and stable nature, MSNs as drug delivery system can protect the biomacromolecules from premature degradation. For most native proteins that are membrane impermeable, MSNs can escort them to cytosol.[145–147] In a example, Lin and co-workers used MSNs with 5.4 nm pore to load cytochrome C and deliver the membrane-impermeable protein into Hela cells via cellular uptake.[148] The enzymes released from MSNs were still highly active in catalyzing its substrate.

Therapeutic genes mainly include short-interfering RNA (siRNA), plasmid DNA and antisense oligomucleotides (ASOs). Compared with viral carriers, non-viral gene delivery systems are much safer and low-immunogenic. The main roadblock of current non-viral carriers is their low gene transfection efficiency. MSNs are considered to be promising candidates for gene delivery with high efficiency. The mesoporous structure and tailorable pore provide room to accommodate gene molecules, which deeply hidden in the mesopores can escape

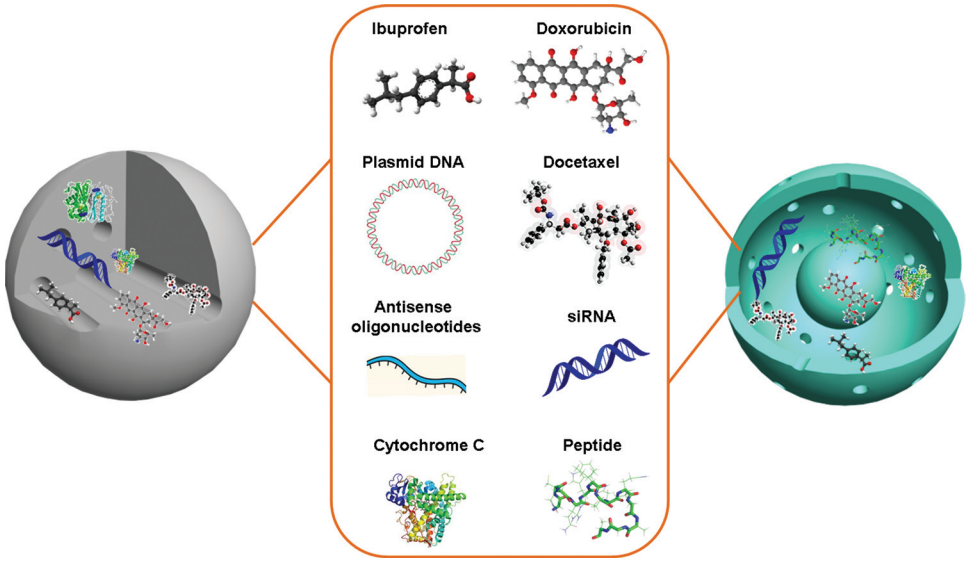

Figure 12. Mesoporous silica nanoparticles as versatile drug delivery systems for a variety of therapeutic agents including pharmaceutical drugs (ibuprofen, doxorubicin, and docetaxel), therapeutic genes (plasmid DNA, antisense oligonucleotides, and siRNA), and therapeutic proteins and peptide (cytochrome C and peptide).

from nuclease degradation during delivery.[149] For increasing the loading capacity of electronegative nuclei acid, the well-established surface chemistry allows easy surface modification of MSNs with polycation. Polycation polymers including polyamidoamine (PAMAM),[150] polyethylenimine(PEI),[151] and mannosylated polyethylenimine(MP)[152] have been used to assemble with MSNs for gene delivery. The positive surface can not only increase the electrostatic interaction between MSNs and negatively charged genes, but also facilitate escape from intracellular endosome by "proton sponge effect". Nel and co-workers found that noncovalent attachment of PEI to the surface of MSNs could not only generate a cationic surface for DNA/siRNA constructs attachment, but also increase MSN cellular uptake.[153] Recently, Gu and co-workers have directly packaged siRNA or DNA within the mesoporous structure of MSNs without any surface modification.[154,155] In this case, the main driving forces for siRNA/DNA adsorption into mesopores were the intermolecular hydrogen bonds instead of electrostatic interaction. Similar to delivery of small pharmaceutical drugs, the loading of genes in MSNs also could be controlled by pore size.[156,157] Min and co-workers synthesized MSNs with very large pores (23 nm) functionalized with amino group for delivering plasmid DNA to human cells.[157] The large pores could protect the plasmid in an intact supercoiled form against degradation by nucleases, whereas plasmid loaded in MSNs with 2 nm pores was completely released or degraded because DNA was mostly on the outer surface of the particles.[157]

Combination therapy with two or more therapeutic agents with complementary or synergistic effect has been used in a variety of disease especially in cancer therapy. It has been one of the hottest areas in nanomedicine to develop efficient drug delivery systems that could simultaneously deliver two or more kinds of therapeutic molecules in a coordinated manner. Because small-molecule drugs and macromolecular drugs differ greatly, conventional drug delivery systems have difficulty in co-delivery. With tunable pore size, MSNs have been proved to be promising drug co-delivery systems.[7,104,139,158,159] They offer both interior pore and exterior particle surface for loading different guest molecules, which is particularly useful for controlling the release sequence of different cargos. Lin and co-workers designed glucose-responsive double delivery system for both modified insulin and cAMP.[7] These two kinds of molecules have precise releasing sequence realizing from immobilizing Gluconic acid-modified insulin (G-Ins) proteins on the exterior surface of MSNs as caps to encapsulate cAMP molecules inside the mesopores. The release of both G-Ins and cAMP from MSNs can be triggered by introduction of saccharides, such as glucose. He and co-workers utilized MSNs to co-deliver doxorubicin and Bcl-2 siRNA into multidrug-resistant cancer cells to reverse the drug resistance.[139] Hanagata and co-workers designed enzyme-triggered drug and gene co-delivery system by combining hollow mesoporous silica with enzyme degradable poly(L-lysine) (PLL) polymer.[159,160] More recently, Brinker and co-workers fused supported lipid bilayer onto MSNs to construct a "protocell" (**Figure 13**A).[104] The organic-inorganic nanocomposites can synergistically combine the advantage of MSNs with extraordinarily high drug loading capacity, and liposome with enhanced lateral bilayer fluidity. They enable targeted delivery and controlled release of high concentrations of multicomponent cargos within the cytosol of cancer cells. The hybrid nanocomposites were used to deliver drugs and drug cocktails, siRNA cocktails and protein toxins (Figure 13B). When delivering a cocktail of DOX, 5-fluorouracil and cisplatin, the protocells have 10^6 times higher kill effect on multidrug resistant cells over comparable liposomes (Figure 13C,D).[104]

4.1.3. Stimuli-Responsive Drug Delivery System (SRDDS)

Most of the pharmaceutical drugs, especially anti-tumoral cytotoxic drugs, have severe toxicity to normal cells. It is not desired

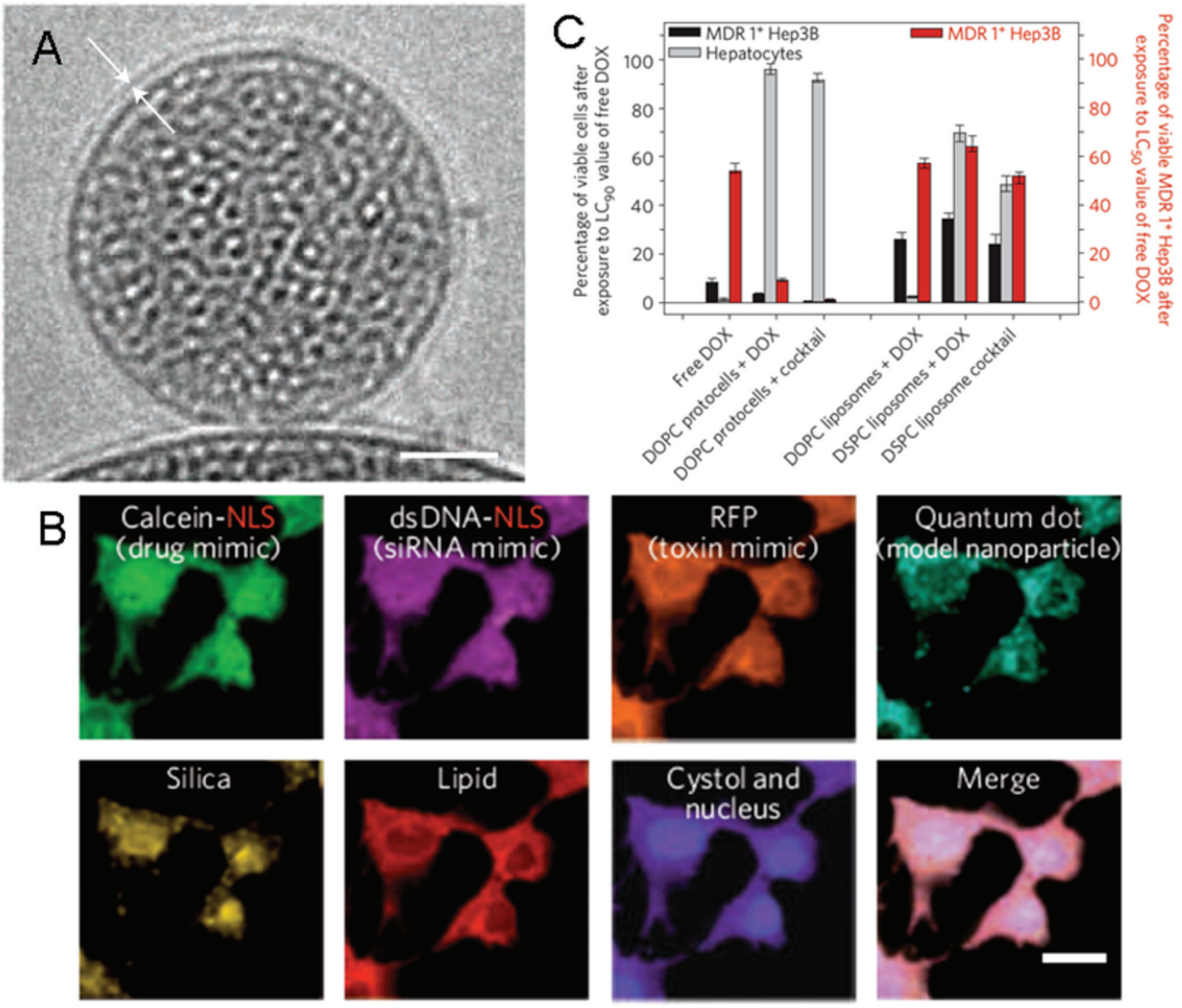

Figure 13. MSN coated with lipid bilayer (called protocell) for multicomponent cargos. (A) Cryogenic TEM image of the protocell. (B) Targeted delivery of multicomponent cargos to the cytosol and nuclei of HCC cells. Alexa Fluor 532-labelled nanoporous silica cores (yellow) were loaded with a multicomponent mixture of four surrogate cargos: calcein (green), Alexa Fluor 647-labelled dsDNA oligonucleotide (magenta), RFP (orange) and CdSe/ZnS quantum dots (teal). Scale bar = 20 μm. (C) Concentration-dependent cytotoxicity of targeting peptide SP94-targeted protocells and liposomes encapsulating DOX. Left axis: the number of MDR1$^+$ Hep3B and hepatocytes that remain viable after exposure to 9.6 μM free DOX, protocell-encapsulated DOX or liposomal DOX for 24 h. Right axis: the number of MDR1$^+$ Hep3B that remain viable after exposure to 2.4 μM free DOX, protocell-encapsulated DOX or liposomal DOX for 24 h. Reproduced with permission from ref. [104]. Copyright 2011, Nature Publishing Group.

that the delivered drugs would be released from drug delivery systems before reaching the disease foci. The so-called "zero premature release" can decrease the drug distribution in off-target sites for decreasing the toxicity and increasing the effective drug accumulation. It also facilitates safe dose-escalation. The stimuli-responsive drug delivery system (SRDDS) can realize a zero premature release in response to external stimuli or internal local microenvironment difference and release the encapsulated drugs into designed locations. MSNs have particular advantages to realize spatio-temporal stimuli-responsive and zero premature release due to their unique drug release mechanism.

In 2003, Tanaka and co-workers first designed a photo-controlled reversible drug release system based on MCM-41.[161] Thy attached a coumarin substituent to the silanol groups of MCM-41, which would yield cyclobutane coumarin dimmers under UV irradiation of 310 nm and obstruct the entrances to the pore of MCM-41. The doors can be reversibly opened when the wavelength of UV irradiation was changed to 250 nm. Afterwards, various photo-stimuli-responsive drug delivery systems have been developed based on the photo-responsive linker including coumarin,[162] thioundecyl-tetraethyleneglycolester-onitrobenzylethyldimethyl ammonium bromide (TUNA),[163] azobenzene derivatives,[164,165] and others.[166] Also in 2003, Lin

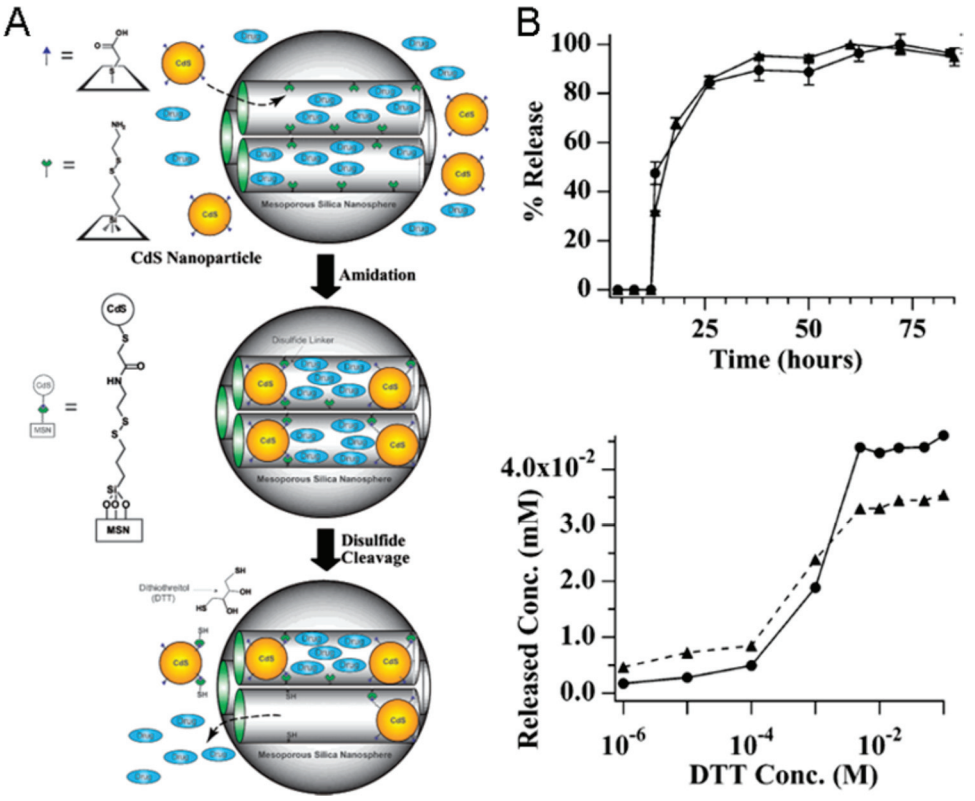

Figure 14. (A) Schematic representation of CdS nanoparticle-capped MSN-based drug delivery system. The controlled release mechanism of the system is based on chemical reduction of the disulfide linkage between the CdS caps and the MSN hosts. (B) the DTT-induced release profiles of Vancomycin (—•—) and ATP (–▲–) from the CdS-capped MSN system. DTT: dithiothreitol. Reproduced with permission from ref. [167]. Copyright 2003, American Chemical Society.

and co-workers used surface-derivatized cadmium sulfide (CdS) nanocrystals as chemically removable caps to encapsulate the drug molecules in the mesopore of MSNs via disulfide linkages between nanocrystals and MSNs (**Figure 14**A).[167] With stimuli molecules of disulfide bond-reducing molecules as trigger, the encapsulated drug molecules can be released from the mesopores (Figure 14B). They also used gold nanoparticles[163] and magnetic nanoparticles[168] as caps. In their other investigations, some other chemical SRDDSs were developed in response to glutathione,[169] disulfide linker cleavage,[168] oligonucleotide,[170] and ATP.[171]

SRDDSs in response to pH,[172–177] ultrasound,[6] temperature,[173,174] redox,[180–183] magnetic field,[184] electric-field,[185] enzymes[186–190] and multi-responsive DDS[191–193] have also been developed. Most of these SRDDSs are based on the reversible opening and closing of mesoporous entrance by particle surface modification and decoration. Because the extracellular pH of tumor tissue is significantly lower than that of normal tissues and there exist some unique enzymes and chemicals, it is beneficial for cancer therapy with the well-designed SRDDSs in response to specific local biological conditions including pH, ionic strength, and enzyme presents.

Up to now, most of these researches are focused on in vitro studies. In recent two years, several works have used the developed SRDDSs for cellular imaging and therapy.[162,169,182,188,194,195] Very few studies have used the SRDDSs for in vivo application.[196] There still have great challenge to remotely manipulate the SRDDS in vivo by photo, magnetic field, or electric field. It is also difficult for SRDDSs to sense the local microenvironment of disease foci, which may have very little difference with peripheral normal tissues in temperature, pH, chemicals, and enzyme catalogue or concentration. Of note, the precondition of developing a clinically applicable SRDDS is all the molecules used to decorate MSN should be biocompatible, and the modification would not result in aggregation of nanoparticles.

4.1.4. Hollow/Rattle-Type Drug Delivery System

Mesoporous silica nanoparticles with a hollow or rattle structure have vast empty spaces to accommodate large quantities of guest molecules, which provides opportunities for a high drug loading capacity. They have both a shell and interior core that can easily be functionalized with desired organic groups, which are favorable for drug loading and targeting delivery. Furthermore, the shell can act as a protective layer to prevent degradation of drugs, especially fragile biomacromolecules. Dependent on the fabrication method, hollow/rattle-type MSNs can be divided into ordered pore particles and disordered, non-oriented counterparts. Ordered straight channels are believed to be favorable for diffusion of absorbed molecules, whereas disordered pore in the shell are considered to be advantageous for controlled and multi-stage drug release.

In 2004, Chen and co-workers first used hollow MSNs to load Brilliant Blue F and cefradine.[197,198] Shi and co-workers proved that the hollow MSNs stored twice as much ibuprofen (744.5 mg/g particle) than conventional MCM-41 type MSNs (358.6 mg/g particle).[199] In the following several years, hollow/rattle-type MSNs have been used as drug delivery systems of fluorescent dye Eosin B Spirit Soluble (ES),[200] ibuprofen,[201] tetracycline,[202] doxorubicin,[177,203–205] L-methionine,[206,207] etc. Hollow mesoporous silica nanoparticles with a composite multilayer structure were also fabricated for drug delivery.[69,208]

Recently, we used the PEGylated silica nanorattle (SN-PEG) to load a water-insoluble antitumoral drug of docetaxel (Dtxl).[209] The drug loading amount was as high as 32% (48 g Dtxl/100 g SN-PEG). It exhibited a low initial burst release (within 10% of the loaded amount) within 60 min and a two-phase drug release behavior. About 80% of the drugs were released within 5 days. We also proved that the silica nanorattle can efficiently load water-soluble drug of doxorubicin with a high loading amount of 18.2%.[210] The doxorubicin showed a pH-sensitive and sustained drug release from the silica nanorattle up to 3 days, with a more rapid drug release rate at pH 4 (close to pH in lysosomes) than at pH 7.4 (pH of blood plasma). The high drug loading amount is beneficial for increasing the drug concentration delivered to cancer cells. The pH-sensitive and sustained drug release behaviors are favorable for drug release from nanoparticles into the cytoplasm of cancer cells following endocytosis.

SRDDSs based on hollow/rattle-type MSNs have been designed in response to pH.[177,211–213] Compared with conventional ordered MSNs, hollow/rattle-type particles present an additional challenge: all of the pores connected to the hollow interior must be controlled. In hollow particles with multiple pore connectivity to the hollow center, absence of control would result in the loss of all of the contents of the particles.[212] Compared with ordered MSNs, development of hollow/rattle-type MSNs is still in its very early stage in terms of both synthesis and applications. Deeper studies are undergoing to make best advantage of hollow structure in biomedical applications.

4.2. Cancer Targeted Therapy

Based on the GLOBOCAN 2008,[214] about 12.7 million cancer cases and 7.6 million cancer deaths are estimated to have occurred in 2008. Cancer has been the leading cause of death in economically developed countries and the second leading cause of death in developing countries. There exists an enormous challenge for preventing and curing cancer at present. Recent advances in nanotechnology have offered new opportunities for cancer prevention, detection and treatment.[11,215] For nano-based cancer targeted therapy, one of the biggest challenges is to achieve sufficiently high local drug concentrations in the tumors, while sparing healthy tissue. The final therapeutic index is determined by biodistribution, metabolism, and clearance of nanoparticulate drug delivery systems. It is also governed by their ability to negotiate biological barriers, penetrate into and accumulate in the tumor tissues. In this part, we discuss the strategies developed for overcoming the in vivo barriers of solid tumor targeted therapy and review recent progresses in MSN-based cancer targeted therapy.

4.2.1. In Vivo Barriers for Cancer Targeting Therapy

Systematically administered nanoparticles would encounter different compartmental barriers before reaching the desired location (**Figure 15**). These barriers are highly efficient for removing foreign materials including nanoparticles from the body. Understanding of these biological barriers is necessary for designing nanoparticles with ability to bypass these barriers and reach cancer cells.

Sequestration of the nanoparticles from the circulation by the reticuloendothelial system (RES) is the most important obstacle. Upon being systematically administered in the body, the nanoparticles would be adsorbed with opsonin proteins in the blood, including complement proteins, laminin, fibronectin, apolipoprotein, thrombospondin, etc., by van der Waals, electrostatic, ionic and other interactions.[216] Subsequently, the absorbed proteins can interact with specific plasma membrane receptors on phaocytic cells and the opsonized nanoparticles would be rapidly removed from the circulation by phagocytic cells especially Kupffer cells in liver and splenic red pulp macrophage (Figure 15A). This is the main clearance pathway for nanoparticles larger than the renal threshold limit of about 10 nm.[217] Macrophage-evading nanoparticles, or so called "stealth nanoparticles" can escape opsonization with a prolonged circulation time. The most efficient method to get stealth nanoparticles is to graft PEG or its derivatives onto the surface of nanoparticles. PEG dynamic chains on the particle surface can not only sterically stabilize particles, but can create a hydrophilic barrier layer to repel protein adsorption. So that the stealth nanoparticles can escape the recognition by phagocytic cells and remain in blood circulation. This is the precondition for the nanoparticulate drug delivery system to be targeted delivered to the tumor along with the blood stream.

After circulating to the desired location, nanoparticles need extravasate from the vasculature into the interstitial space of solid tumor tissue. The abnormal vascular structure of tumor endows substantial advantages for nanoparticulate drug delivery systems with sizes ranging from around 30 to 400 nm for passive tumor targeting.[218] That is, the tumor tissue has extensive tumor angiogenesis with abnormal vascular architecture, which contains a discontinuous or absent basement membrane and impaired lymphatic drainage (Figure 15B). It allows for large macromolecules and small nanoparticles to extravasate and accumulate in the interstitial tumor space. The so-called enhanced permeability and retention (EPR) effect has been considered as the key rationale for passive targeting of nanoparticles. Particle size, hydrophobicity/hydrophilicity, and surface chemistry of nanoparticles would greatly influence the vascular permeability of the transported nanoparticles.[12,219] However, nanoparticles could also be leaked into inflammation locations with increased vessel permeability. Moreover, the leaky properties of tumor vasculature are not always existent. It is related to tumor type and development stage, which is quite different from patient to patient. Even though with EPR effect, difficulties still exist for uniform delivery of the nanoparticles to all regions of tumor tissue. Homogenous distribution of nanoparticles and therapeutic agents in tumor tissues is impeded by

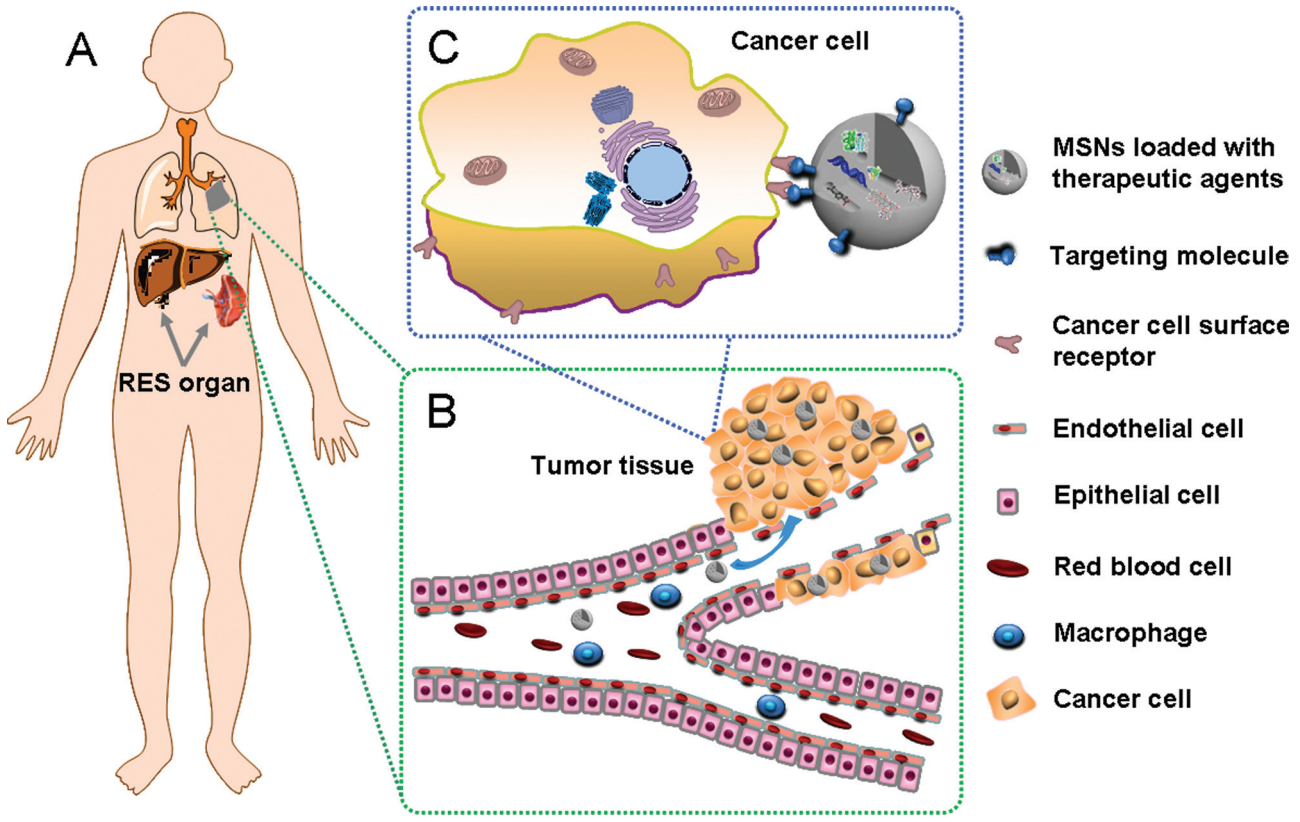

Figure 15. In vivo barriers encountered by nano-based drug delivery system after systematic administration for cancer therapy and the nano-based strategies developed for cancer targeted therapy.

elevated intratumoral interstitial fluid pressure, dense extracellular matrix, lack of convection and existence of poorly perfused hypoxic regions.

The potential limitations of passive targeting promote the development of more advanced active targeting. Because of the high metabolic demands for rapid proliferation, cancer cells generally overexpress folate and transferrin receptors. Bioconjugation of folate and transferrin (Tf) or antibodies of these receptors to the surface of nanoparticles can actively deliver the nanoparticles to cancer cells. However, folate and transferrin receptors are also ubiquitously expressed on normal cells.[220] For example, transferrin receptors (TfR) is overexpressed on normal cells with high proliferation rate and those requiring large amounts of iron. It is also highly concentrated in brain capillary endothelium for mediating the iron transport across the blood-brain barrier (BBB). For more active targeting, nanoparticles are bioconjugated with specific antibodies, peptides, ligands, aptamers, and oligonucleotides that can specifically and selectively bind with receptors expressed or overexpressed on certain cancer cells (Figure 15C). Another strategy is to attach specific ligands that can specifically associate with receptor on tumor vascular endothelial cells. Arginine-glycine-aspartate (RGD) containing peptides, which bind to $\alpha_v\beta_3$-integrin overexpressed on angiogenic endothelial cells, are widely used for selectively targeting angiogenesis. However, the considerable development could not circumvent the problem of limited penetration of the nanoparticles into the deeper region of cancer tissues.[12] More efficient targeting strategies are expected for higher targeting efficiency and deeper penetration into tumor tissues.

After delivered into tumor interstitium, the nanoparticles should enter into cancer cells and release the payloads to desired subcellular organelles, or cytosol. The cellular barriers that should be conquered include penetration of cell membrane, escape from endosome, and penetration of nuclear membrane, etc. Small and hydrophobic drug molecules can enter cells by passive permeation across the lipid bilayers, whereas other drugs are difficult to cross the cellular membranes by themselves. Nanoparticles facilitate the drugs enter into cells by endocytosis, which is an energy dependent process including phagocytosis, macropinocytosis, clathrin-mediated endocytosis and caveolae-mediated endocytosis. The endocytic rate, amount and pathway depend on cell type and particle size, shape and surface chemistry. Although some studies have reported that the active targeting nanoparticles did not show increased accumulation in tumor tissues, it is definite that bioconjugation of targeting ligands onto particles can help increase the cancer cellular uptake and enhance the cellular killing effect with increased intracellular drug concentration.[221] After endocytosed, the nanoparticles would enter into different subcellular organelles such as caveosomes and endosome/lysosome. In the acidic organelles, the nanocarriers act as protector for drugs especially therapeutic molecules with low inherent stability. Most of the nanoparticles would end up in lysosomes. To enter

into cytosol or nucleus, the uptaken nanoparticles must escape from the lysosomes. Nanoparticles designed with buffer capacities in response to the acidification of endosomes/lysosomes could escape from the endosomes/lysosomes and deliver drugs to cytosol via "proton sponge" effect.[222]

4.2.2. Targeting Therapy Using MSN-Based Drug Delivery System

Tremendous efforts have been made using MSNs as drug delivery systems for cancer-targeted therapy. Although it was reported that 50 and 250 nm silica nanoparticles had higher blood distribution and higher blood/liver ratio than PEGylated solid lipid nanoparticles and polycyanoacrylate nanoparticles,[223] more results with the opposite outcome were reported.[101,102] To decrease RES uptake and maximize the EPR effect, Nel, Zink and co-workers coated 50-nm MSNs with PEI-PEG copolymer to reach a high passive accumulation of about 12% at the tumor site, compared with 1% of 100 nm phosphonate-coated MSN and 3% of 50 nm PEGylated MSNs (**Figure 16**A). The increased tumor accumulation further brought an enhanced tumor inhibition rate (Figure 16B-C).[224] The additional cationic polymer coated on the MSNs increased the steric hindrance between nanoparticles for improved particle stability. Currently, the tumor passive targeting efficiency in mice is lower than 10% in most reported results.[225,226] It is still a challenge to further increase the in vivo circulation time and the passive targeting efficiency for MSN-based drug delivery systems.

We designed PEGylated silica nanorattles with a diameter of 125 nm as nanocarriers of docetaxel (Dtxl) for liver cancer therapy (**Figure 17**A).[65] With high loading capacity, passive targeting ability and decreased off-target distribution, the silica nanorattle encapsulated Dtxl showed 15% increased tumor inhibition rate (Figure 17B) compared with Taxotere, the clinical formulation of docetaxel. Meanwhile, silica nanorattle encapsulated Dtxl had significantly decreased liver toxicity and hematological toxicity (Figure 17C,D).

By bioconjugating MSNs with specific targeting ligands, active targeting to cancer cells or angiogenic endothelial cells has been realized. The targeting ligands now used for active targeting of MSN-based DDS include folate for targeting folate receptor,[9,227–230] transferrin for targeting transferrin receptor,[231] aptemer sgc8 for targeting PTK7 (human protein tyrosine kinase-7) overexpressed in colon carcinomas,[232] antibody for targeting Her-2 receptor overexpressed in breast or lung cancer,[233] and cyclic-RGD for targeting $\alpha_v\beta_3$ integrin. Similar to the importance of molecule weight and grafting density of PEG for passive targeting, the property and grafting density of targeting ligands on particle surface are significant for active targeting, which have now been paid little attention for MSN-based drug delivery systems and should be critically researched. First, it should select the active targeting ligands with high specificity but suitable affinity to their receptors for a given tumor type.[221] Low affinity would result in suboptimal targeting efficiency, whereas extraordinarily high affinity would induce low tumor penetration ability because of the strong tendency of ligands to be sequestered by the tumor cells near blood vessels. Second, the grafting density of ligands onto nanoparticles should be carefully designed. Multivalent binding can increase the avidity between ligands and receptors for multiple interactions, but multivalent ligands presentation may increase the immunogenicity and recognition of nanoparticles by RES.[14] Third, the bioconjugation of ligands should not influence the dispersity of the nanoparticles. Forth, interaction between nanoparticles and ligands should be stable before the nanoparticles reach tumor site.

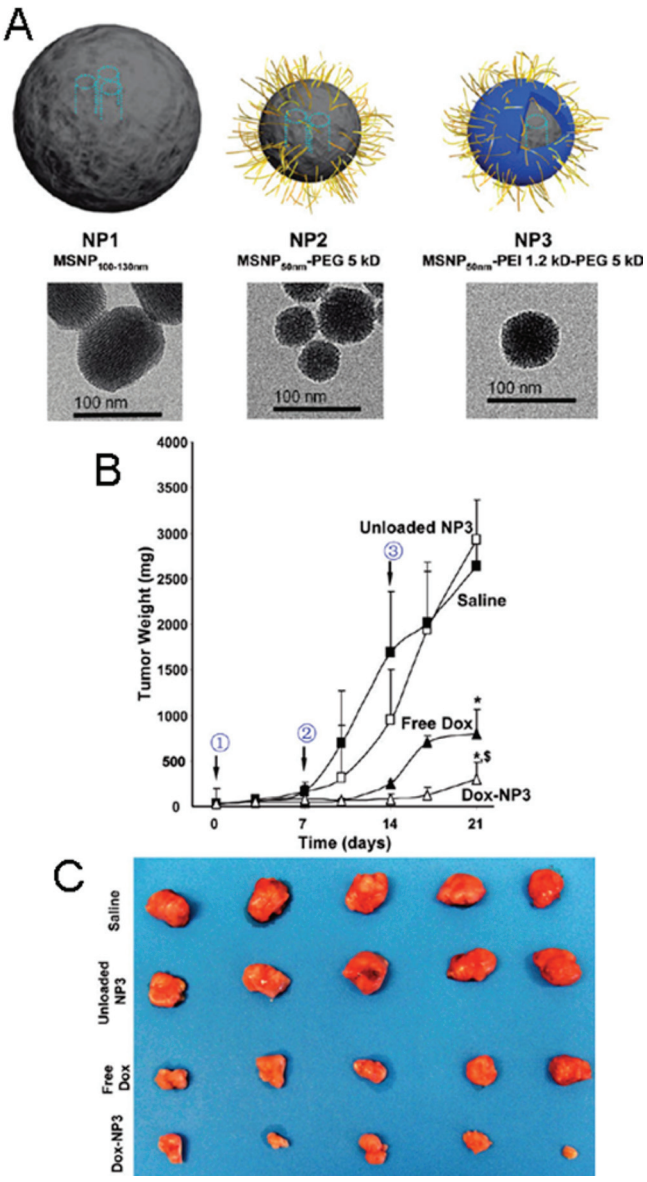

Figure 16. (A) Graphical representation and TEM image of modification of mesoporous silica particle. NP1: phosphonate-coated MSN with a primary particle size of 100 nm. NP2: PEGylated mesoporous silica with core size of 50 nm. NP3: 50 nm MSNs coated with PEI-PEG. (B) Comparison of the tumor inhibition effect of doxorubicin-loaded NP3 (Dox-NP3) versus free drug (free Dox), empty particles, and saline in the KB-31 xenograft model and (C) corresponding photograph of the tumor tissue at the end of therapy. Reproduced with permission from ref. [224]. Copyright 2011, American Chemical Society.

After targeted to tumor tissues, MSNs can enter into cancer cells via energy-dependent cellular uptake.[234] The cellular uptake capacity of nanoparticles can be tuned by changing

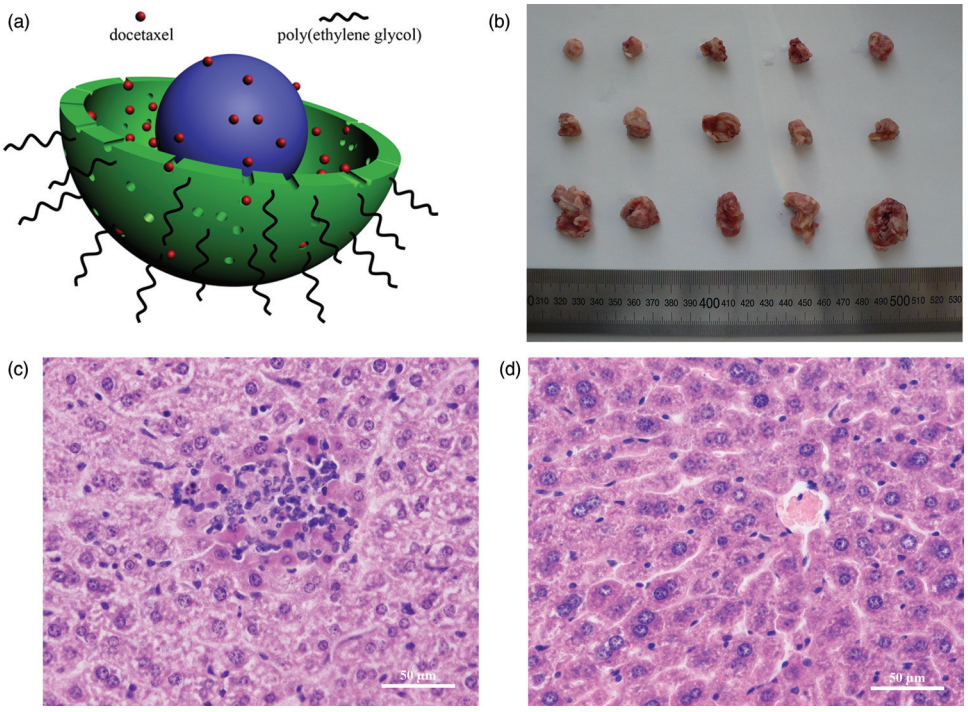

Figure 17. Silica nanorattles as drug delivery system of docetaxel for liver cancer therapy with low toxicity and high efficacy. (A) Schematic diagram of the drug delivery system based on silica nanorattles for docetaxel. (B) In vivo antitumor activities of SN-PEG-Dtxl and Taxotere (clinical formulation of docetaxel) on H22 liver cancer subcutaneous model. Photographs of tumors after therapy from a) SN-PEG-Dtxl group, b) Taxotere group, and c) control group. Systematic toxicity of Taxotere and SN-PEG-Dtxl on healthy ICR mice. Histological section stained with H&E of liver samples of (C) SN-PEG-Dtxl and (D) Taxotere group. H&E: hematoxylin and eosin. Reproduced with permission from ref. [65]. Copyright 2010, American Chemical Society.

particle size,[78] surface properties,[95,153] and surface bioconjugation with ligands specifically binding with cellular receptor.[233] After entering into cells, the nanoparticles would release the loaded chemotherapeutic drugs or therapeutic macromolecules, which have different mechanisms to kill cancer cells and need be delivered into corresponding subcellular organelles. For instance, our results showed that the PEGylated silica nanorattles have a high efficiency to escape from the lysosomes to the cytosol for releasing loaded Dtxl into cytosol. Dtxl can bind with β-tubulin and stabilize microtubules to induce cell-cycle arrest and apoptosis.[65] For doxorubicin, it would associate with DNA for desired tumor cell apoptosis.[235]

Although the passive and active targeting have been designed, targeting efficiency is not as ideal as expected. Recently, an efficient approach for tumor-targeted drug delivery with mesenchymal stem cells as targeting vehicle and silica nanorattle as drug carrier has been developed.[235] With the tumor-tropic property of mesenchymal stem cells (MSCs) towards malignant cells,[236] it is hypothesized that attachment of nanoparticles to MSCs may be a promising strategy for actively directing the drug-loaded nanoparticles into tumor. A silica nanorattle-doxorubicin drug delivery system was efficiently anchored to MSCs by specific antibody-antigen recognition at the cytomembrane interface (**Figure 18**A). Up to 1500 nanoparticles can be uploaded to each MSC with high cell viability and tumor-tropic ability. The burdened MSCs can track down U251 glioma tumor cells more efficiently and deliver doxorubicin with wider distribution and longer retention lifetime in tumor tissues compared with free DOX and silica nanorattle-encapsulated DOX (Figure 18B). The increased and prolonged DOX intratumoral distribution further significantly enhanced tumor-cell apoptosis (Figure 18C). The results provide us a robust and generalizable strategy for cancer targeted therapy with high efficiency and low systematic toxicity.

No matter which targeting strategy to use, the particle size, shape and surface property of MSNs have a profound impact on the ability of particles to overcome the in vivo biological barriers, reach tumor tissue, enter into tumor cells, and release loaded therapeutic agents for therapy. The relationship between these physiochemical properties of nanocarriers and the tumor targeting efficiency should be further studied. Improvement of the knowledge of cancer physiopathology, discovery of new targets and development of new targeting ligands are most significant challenges for improving nano-based cancer targeted therapy from the aspect of cancer biology.

4.2.3. Overcome the Multidrug Resistance

Multidrug resistance (MDR) is the most important impediment for successful chemotherapy even with targeted drugs or/and combination chemotherapy. In cancer chemotherapy, often drug-sensitive cells are killed, but a proportion of drug-resistant cells are left. The remaining cancer cells would grow again and result in tumor relapse and metastases. Generally, the multidrug

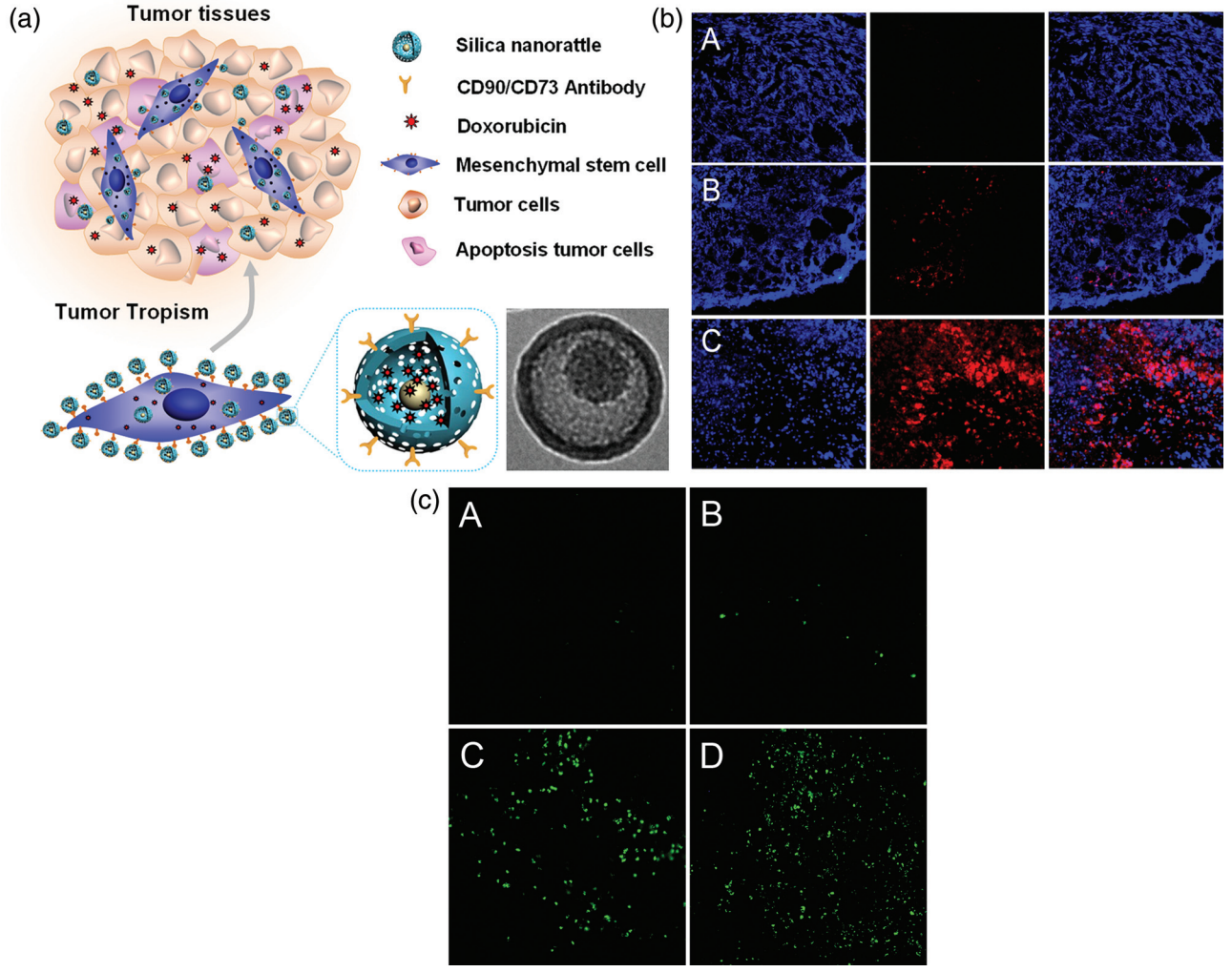

Figure 18. (A) Schematic illustration of silica nanorattle-doxorubicin-anchored mesenchymal stem cells (MSC-SN-Ab(CD90)-DOX) for tumor-tropic therapy. (B) Fluorescent microscopy images of tissue sections 7 days after intratumoral injection of a) DOX, b) SN-DOX, and c) MSC-SN-Ab(CD90)-DOX. Blue fluorescence shows nuclear staining with DAPI and red fluorescence shows the location of doxorubicin. C) TUNEL staining assay showing cell apoptosis by a) control, b) DOX, c) SN-DOX, and d) MSC-SN-Ab(CD90)-DOX at 7 days after intratumoral injection. Reproduced with permission from ref. [235]. Copyright 2011, American Chemical Society.

resistance mechanism can be grouped into at least five categories: increased drug efflux, decreased drug influx, activation of DNA repair, activation of anti-apoptotic pathways and activation of detoxifying systems (**Figure 19**). As the predominant mechanism of multidrug resistance, increased drug efflux is mediated by ATP-dependent efflux pumps, typically of the ATP-binding cassette (ABC) superfamily. The ATP-dependent transporters can expel delivery of antitumor drugs into tumor cells and significantly decrease the intracellular drug accumulation.[237] Non-pump resistance by activation of anti-apoptotic pathways can suppress the cell apoptosis and improve cell survival. It often involves the genetic and epigenetic alterations of cancer cells including overexpression of Bcl-2 (B-cell lymphoma 2, an anti-apoptosis regulator protein) and mutations in tumor suppressor p53 gene. For recent years, it has been recognized that cancer could not be simply viewed as the traits of the cancer cells.[238] The existence of cancer stem cells (CSCs) or called tumor initiating cells and the tumor microenvironment or named tumor niche also play significant roles in maintenance and development of drug resistance.[239]

Nanoparticulate drug delivery systems can facilitate cellular uptake, increase intracellular accumulation and decrease cellular efflux in drug-resistant cancer cells. The process is realized by energy-dependent active cellular uptake of nanocarriers for bypassing drug efflux pumps. However, it is not sufficient for overcoming the drug resistance. Considering the mechanism of drug resistance, the drug resistance can be reversed by decreasing the expression or suppressing the activity of ATP-dependent transporters via gene knockdown or pharmaceutical inhibitors respectively. Nano-based drug co-delivery systems have been designed for targeting the ATP-dependent transporters concurrently delivering chemo-drugs for increasing intracellular drug concentration.[240] It is also possible to co-deliver cytotoxic drugs and genes targeting non-pump resistant related molecules including Bcl-2,[139] transcription factor NF-κB and hypoxia-inducible factor alpha (HIF-1α).[241]

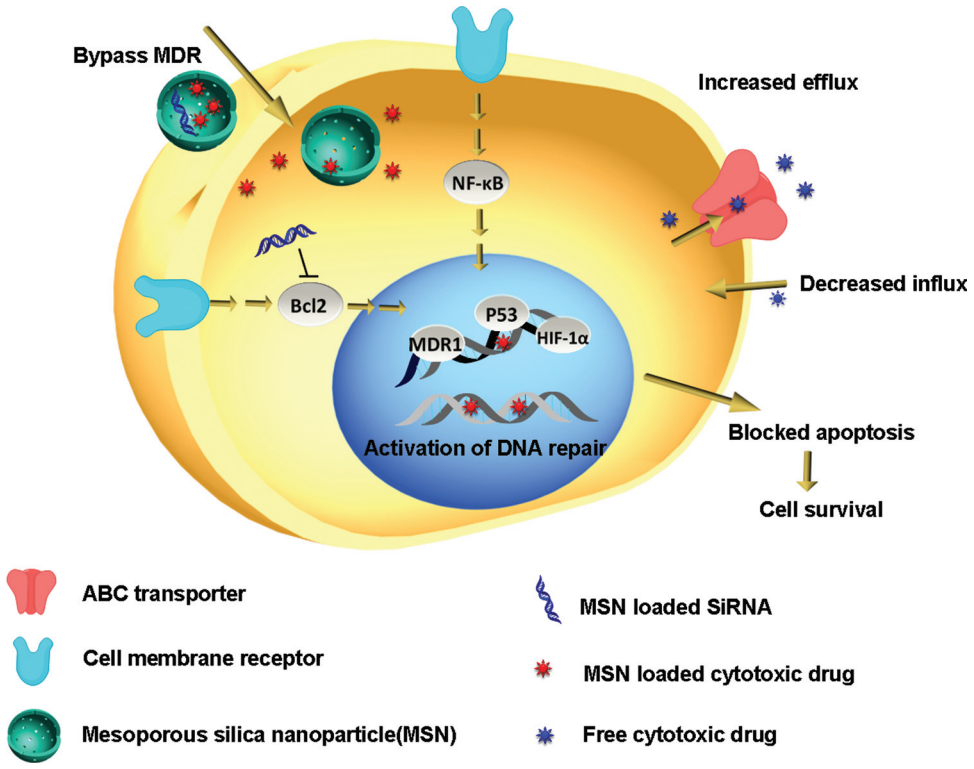

Figure 19. Schematic illustration of cancerous multidrug resistance and strategies for overcoming MDR. Drug-resistant cancer cells have several pathways to evade the cytotoxic drugs including deceased drug influx, increased drug efflux by overexpressed ABC transporters, activation of DNA repair, and inhibition of drug-induced apoptosis. The anti-apoptotic signaling pathways always involve overexpression of Bcl-2, activation of MDR1, NF-κB, and HIF-1α, and mutation of tumor suppressor p53 gene. MSNs can be internalized into the drug-resistant cancer cells for bypassing the multidrug resistance. Upon endocytosis, the loaded cytotoxic drugs could be sustainedly released into cells, and the loaded siRNA targeting related gene could reduces drug resistance.

One of the advantages of MSNs over other nanocarriers for killing drug-resistant cancer cells is their extraordinarily high drug loading capacity, which can significantly increase the intracellular drug concentration under a situation of limited cellular uptake of nanoparticles. It was reported that with a 1000 times higher drug loading capacity over liposomes, doxorubicin loaded protocells (lipid bilayer coated MSNs) showed comparable toxicity to drug resistant hepatocellular carcinoma cells than 10^5 time amount of liposomal doxorubicin.[104] Another intriguing advantage of MSNs is the co-delivery ability of several different kinds of therapeutic agents with complementary or synergistic effect. MSNs as drug co-delivery systems have been designed for co-delivery of chemotherapeutic drug and siRNA silencing ABC transporters gene MDR1,[242] chemotherapeutic drug and siRNA silencing Bcl-2 gene,[139] and chemotherapeutic drug and surfactant chemosensitizer.[243] With the synergistic effect, the intracellular drug accumulation can be greatly increased and subsequently induce increased therapy efficacy. In one instance, by co-delivering Bcl-2 siRNA and DOX, it can increase the anticancer efficiency for 132 times to drug resistant human ovarian cancer cells compared with free DOX.[139] Notch signaling plays significant role in tumor angiogenesis, maintenance and progression, and is a specific cancer stem cell signaling for maintaining stem cell characteristics.[244] Lindén and co-workers have delivered γ-secretase inhibitors (GSIs) encapsulated into folate bioconjugated PEI coated MSNs to inhibit the Notch signaling, which showed effective Notch inhibition and significantly enhanced breast tumor therapy efficacy.[245]

Of note, despite significant achievements have been made, the mutability and heterogeneity of cancer cells will always provide them with versatile ways to evade the drugs, no matter how new the anticancer drugs. It still relies on further thorough understanding of the physiological mechanisms of drug resistance for increasing the nano-based cancer therapy. It is expected that an "Achilles heel" could be found against drug-resistant cancer cells.

4.3. Multifunctional Nanocomposites Based on MSNs

With its abundant surface silanol groups, a mesoporous structure, and the facile sol–gel synthetic method, silica provides a matrix for integrating other nanoparticles/chemicals to form nanocomposites, which has been widely used as coating materials to increase the stability and biocompatibility of nanoparticles.[246] More importantly, nanocomposites that integrate semiconductor, metal, and metal oxide nanoparticles with special optical, magnetic, and electronic properties hold promise for cancer diagnosis and theranostics. Fabrication methods including microemulsion methods,[247] coating methods,[248–251]

and post-synthetic treatment,[252,253] etc. have been designed to synthesize multifunctional MSN including Fe_3O_4@MSN,[247,250,252,254,255] Gd-Dye@MSN,[248] Fe_3O_4-Dye@MSN,[251] and Fe_3O_4/QD@MSN.[249] In the synthesis of multifunctional nanocomposites several factors must be taken into consideration: the fabrication process should not be too complex, the particle formation should not be too expensive, and the prepared nanocomposites should be stable and well dispersed.

The nanocomposites have multifunctions for simultaneous therapy and diagnosis with Fe_3O_4 nanoparticles as T_2 magnetic resonance imaging (MRI) contrast agents, paramagnetic complexes of Gd compound as T_1 MRI contrast agents, semiconductor quantum dots/fluorescent dyes for fluorescent imaging (FI), and plasmonic nanomaterials for photothermal therapy. MRI has been widely used in clinics for its high spatial resolution and capacity to obtain physiological and anatomical information simultaneously, while more and more attention has been paid to FI due to its high sensitivity and rapid screening capacity. Integration of these two imaging modalities into one mesoporous silica nanoparticle as a dual-modality contrast agent could be used in a single clinical procedure for pre- and post-operative MRI and intraoperative FI, providing enhanced imaging before, during, and after the procedures (**Figure 20**).[251,256,257] Integrated theranostics by integrating multiple imaging agents into one single mesoporous silica nanoparticle with concurrent drug delivery can monitor the treatment process in real-time, detect the biodistribution of nanoparticles, and confirm the foci area and margin, which offer great promise for personalized therapy.[13,68,258–260] Especially when bioconjugating targeting ligands onto MSNs[250,261] or manipulating the magnetic nanocomposites under external magnetic field,[262] the nanoparticles can specifically find the tumor tissue for targeted theranostics.

Plasmonic nanomaterials as strong near-infrared (NIR) light absorbing agents have provided new opportunities for localized hyperthermia therapy. We have synthesized multifunctional gold nanoshell on silica nanorattles (pGSNs) for therapy of hepatocellular carcinomas by combining photothermal therapy with chemotherapy.[67] Silica nanorattles with positive changed surface greatly simplified the gold nanoshell coating process without using any silane coupling agents (e.g., APTMS) modification.[263] The combination of hyperthermia and chemotherapy is an encouraging approach which induces synergistic effect that is greater than the two treatments alone (**Figure 21**B). Most recently, we engineered transferrin and PEG functionalized gold nanoshell on silica nanorattle (pGSN-Tf) loaded with docetaxel (pGSNs-Dtxl-Tf) for targeted ablation of breast carcinoma (Figure 21C).[264] Via a single NIR light irradiation, the in vivo breast tumors showed complete regression by combination of selectively targeting, photothermal therapy and chemotherapy (Figure 21D). We believe this kind of multifunctional nanoformulation can be regarded as a 'magic bullet', providing a highly efficient, lowly toxic and minimally invasive treatment via single-dose treatment.

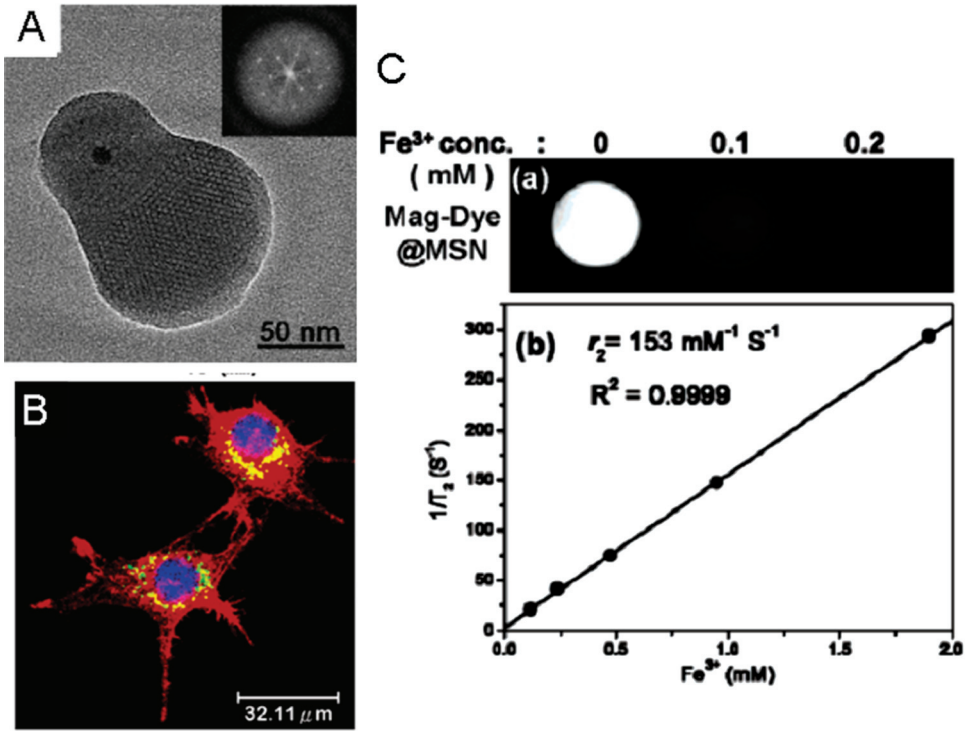

Figure 20. Tumblerlike mesoporous silica nanocomposites (Mag-Dye@MSN) with magnetic, luminescent, and mesoporous properties. (A) HR-TEM and fourier transform pattern of Mag-Dye@MSN. (B) Fluorescent imaging of Mag-Dye@MSN uptaken by NIH 3T3 cells (green). Red: cell skeleton stained with rhodamine phalloidin; Blue: cell nucleus stained with DAPI. (C) T_2-weighted MR images of an aqueous suspension of Mag-Dye@MSN taken at 4.7 T on a Biospec spectrometer; (b) T_2 relaxivity plot of an aqueous suspension of Mag-Dye@MSN measured at 0.47 T on a Minispec spectrometer. Reproduced with permission from ref. [256]. Copyright 2006, American Chemical Society.

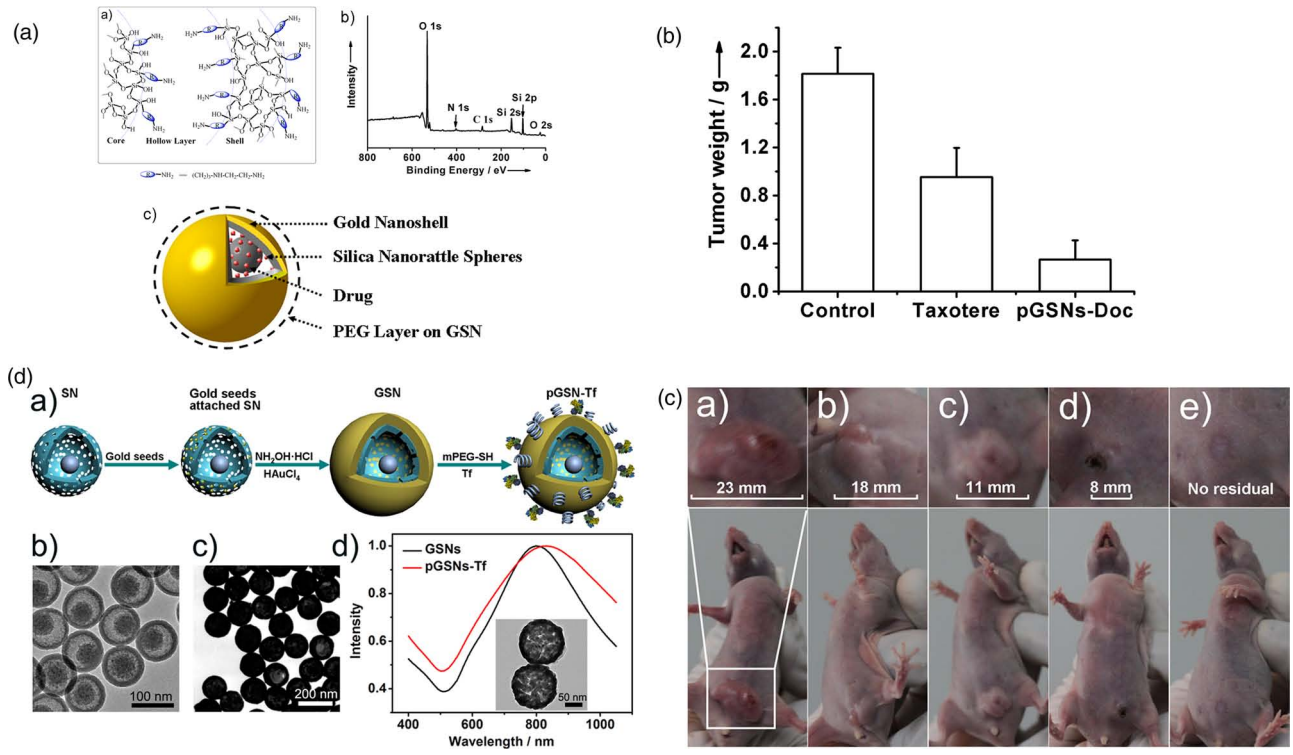

Figure 21. Gold nanoshell on silica nanorattle (GSN) for synergistic therapy of hepatocellular carcinomas by combination of photothermal therapy and chemotherapy. (A) Synthesis of gold nanoshell on silica nanorattle. a) Structure of the silica nanorattle with positively charged surface, b) X-ray photoelectron spectroscopy (XPS) of silica nanorattle proving the existence of free amino groups on particle surface, and c) PEGylated gold nanoshell on silica nanorattle(pGSN) as drug delivery system. (B) In vivo antitumor activities of pGSN-Dtxl on H22 liver cancer subcutaneous model. (A-B) Reproduced with permission from ref. [263] Copyright 2010, Wiley. (C) a) Synthesis of transferrin tethered pGSN-Dtxl for targeted therapy of breast cancer, b) TEM image of silica nanorattles, c) TEM image of GSNs, and d) extinction spectra of pGSNs and pGSNs-Tf. The inset is the TEM image of pGSNs-Tf.[264] (D) In vivo targeting therapy of MCF-7 bearing nude BALB/c mice. Photographs at day 17 of representative mice from groups of a) control, b) pGSNs-NIR, c) Texotere, d) pGSNs-Dtxl-NIR, e) pGSNs-Dtxl-Tf-NIR. (C-D) Reproduced with permission from ref. [264]. Copyright 2012, Wiley.

5. Conclusion and Outlook

In conclusion, we have reviewed the ten-year progress in synthesis, biocompatibility research, and drug delivery application of mesoporous silica nanoparticles. As summarized, MSNs with their versatile mesoporous structure have unique advantages that may allow clinically applicable nanoformulations for disease diagnosis and therapy. First, MSNs can be tailored in size, surface chemistry, shape, and mesoporous or hollow structure. As drug delivery systems, they have an extraordinarily high drug loading capacity and stimuli-responsive drug release profiles. Second, MSNs have relatively high in vitro and in vivo biocompatibility and could eventually be excreted from the body. Third, the ease of multifunctionalization with magnetic, fluorescent, and photothermal properties allows simultaneous bioimaging and drug delivery for nanotheranostics. Fourth, the flexible, scalable, and cost-effective fabrication of MSNs provides unique opportunities for future industrial production and clinical translocation. Overall, MSNs are excellent candidates for use in drug delivery systems. Nonetheless, as a relatively new and burgeoning application in nanomedicine, a lot of questions still need to be addressed before clinical application.

First, biomedical application in drug delivery depends on the well-controlled fabrication of nanomaterials. It is important to synthesize well-defined MSNs and drug loaded counterparts with tailorable size, shape, structure, pore geometry, and surface properties. The synthesis method should be simple, stable, cost-effective, and scalable for facilitating future industrial production and clinical translocation. Second, establishment of the host-guest interaction of MSNs with therapeutic agents could help to fully utilize the mesoporous and/or hollow structure for drug encapsulation with high drug payloads and rational release profile. Third, prior to be implemented in clinical practice, we need extensive preclinical studies including more complicated chemophysical characterizations of the synthesized MSNs and their related effects on biotranslocation and biocompatibility. In addition to acute toxicity, research on subchronic and chronic toxicity, as well as the change in molecular level (such as genotoxicity) caused by systematically administered MSNs should not be neglected. A recent report has shown that 35-nm and 70-nm non-porous silica nanoparticles could cause pregnancy complications when injected intravenously into pregnant mice.[265] Would MSNs with similar diameter cause similar toxicity? It alarms us to perform a more cautious and thoughtful toxicity

evaluation of the intentionally exposed MSNs. Better understanding of the toxicity aspect not only allows a better estimation of the potential risk, but could also balance the efficacy and safety by selecting a suitable dosage with maximal therapeutic benefit and minimal toxic effect.

For cancer therapy, MSNs show obvious advantages over other nanoparticulate drug delivery systems because of their extraordinarily high drug loading, controlled drug release behavior, and co-delivering ability. However, great challenges still exist. To overcome the in vivo physiological barriers and achieve efficient delivery of nanoparticles to cancer cells, MSNs as nanocarriers should integrate the properties of long circulation time, low RES sequestration, ability to extravasation into tumor tissue, and specific cancer cell internalization. The properties of nanoparticulate drug delivery systems and the physiological microenvironment in bodies co-determine the final therapeutic benefits. Even if with efficient delivery to tumor site, the physiological nature of cancer brings tremendous difficulties in efficient therapy. Cancer multidrug resistance is a dynamic systemic result including multiple molecular, cellular and microenvironmental aspects. It may hold promise for conquering MDR by targeting DDS to the molecular foundation responsible for MDR development, to the population of cancer stem cells, and to the tumor niche. On the other hand, tumor is highly dynamic and heterogeneous, which can adapt readily to imposed stress. Thus, it is impossible that a single formulation could be effective to every population of patients at any time. With the diversity and multifunctionality of MSN-based nanocomposites, it is promising way to develop cooperative therapies such as utility of the synergistic effect of photothermal/magnetohyperthermal therapy and chemotherapy, or simultaneous utility of several nano-based formulations targeting different population of cancer cells with different phenotype. Certainly, more knowledge about cancer biology and physiology from biologist is essential for more specific targeting options.

In conclusion, the research on MSNs for biomedical applications is taking off. Tremendously positive research results encourage further exploration. It is encouraging that a kind of ultrasmall multimodal silica nanoparticles (Cornell dots, C dots) has recently been approved by the FDA for the first-in-human clinical trial for targeted diagnostics of advanced melanoma.[266,267] Nevertheless, it is still a long way to translate the formulations of MSN-based drug delivery systems into the clinical market because sufficient evidence needs to be accumulated to prove the safety and therapeutic efficacy. In addition to scientific efforts, commercial and social drive are also a fundamental requisite. It requires leveraging resources and expertise from a multitude of disciplines including chemistry, materials science and engineering, biology, pharmaceutical sciences, and clinical/translational research. It is expected that with multidisciplinary efforts for the common objective of clinical benefits, MSN-based nanoformulations can make an exciting breakthrough and direct a renovated individualized therapy in the near future.

Acknowledgements

The work was supported by National Nature Science Foundation (81171454, 30900349, 60736001). The authors thank Mr. Nanjing Hao for the preparation of the scheme, and Dr. Huiyu Liu, Dr. Tianlong Liu, Dr. Longfei Tan for useful discussions.

Received: December 13, 2011
Published online: February 29, 2012

[1] M. Vallet-Regí, A. Rámila, R. P. del Real, J. Pérez-Pariente, *Chem. Mater.* **2001**, *13*, 308.
[2] D. Lozano, M. Manzano, J. C. Doadrio, A. J. Salinas, M. Vallet-Regí, E. Gómez-Barrena, P. Esbrit, *Acta Biomater.* **2010**, *6*, 797.
[3] M. Zhu, H. X. Wang, J. Y. Liu, H. L. He, X. G. Hua, Q. J. He, L. X. Zhang, X. J. Ye, J. L. Shi, *Biomaterials* **2011**, *32*, 1986.
[4] M. Vallet-Regí, *Chem. Eur. J.* **2006**, *12*, 5934.
[5] A. Suwalski, H. Dabboue, A. Delalande, S. F. Bensamoun, F. Canon, P. Midoux, G. Saillant, D. Klatzmann, J. P. Salvetat, C. Pichon, *Biomaterials* **2010**, *31*, 5237.
[6] H. J. Kim, H. Matsuda, H. S. Zhou, I. Honma, *Adv. Mater.* **2006**, *18*, 3083.
[7] Y. N. Zhao, B. G. Trewyn, I. I. Slowing, V. S. Y. Lin, *J. Am. Chem. Soc.* **2009**, *131*, 8398.
[8] B. Moulari, D. Pertuit, Y. Pellequer, A. Lamprecht, *Biomaterials* **2008**, *29*, 4554.
[9] J. Lu, M. Liong, Z. X. Li, J. I. Zink, F. Tamanoi, *Small* **2010**, *6*, 1794.
[10] D. Peer, J. M. Karp, S. Hong, O. C. FaroKHzad, R. Margalit, R. Langer, *Nat. Nanotechnol.* **2007**, *2*, 751.
[11] V. Wagner, A. Dullaart, A. K. Bock, A. Zweck, *Nat. Biotechnol.* **2006**, *24*, 1211.
[12] R. K. Jain, T. Stylianopoulos, *Nat. Rev. Clin. Oncol.* **2010**, *7*, 653.
[13] W. R. Sanhai, J. H. Sakamoto, R. Canady, M. Ferrari, *Nat. Nanotechnol.* **2008**, *3*, 242.
[14] E. Ruoslahti, S. N. Bhatia, M. J. Sailor, *J. Cell. Biol.* **2010**, *188*, 759.
[15] N. J. Halas, *ACS Nano* **2008**, *2*, 179.
[16] A. E. Garcia-Bennett, *Nanomedicine-UK* **2011**, *6*, 867.
[17] T. Yanagisawa, T. Shimizu, K. Kuroda, C. Kato, *Bull. Chem. Soc. Jpn.* **1990**, *63*, 988.
[18] C. T. Kresge, M. E. Leonowicz, W. J. Roth, J. C. Vartuli, J. S. Beck, *Nature* **1992**, *359*, 710.
[19] Y. Wan, D. Y. Zhao, *Chem. Rev.* **2007**, *107*, 2821.
[20] F. Hoffmann, M. Cornelius, J. Morell, M. Fröba, *Angew Chem. Int. Edit.* **2006**, *45*, 3216.
[21] I. I. Slowing, J. L. Vivero-Escoto, B. G. Trewyn, V. S. Y. Lin, *J. Mater. Chem.* **2010**, *20*, 7924.
[22] H. P. Lin, C. Y. Mou, *Acc. Chem. Research* **2002**, *35*, 927.
[23] Q. Cai, Z. S. Luo, W. Q. Pang, Y. W. Fan, X. H. Chen, F. Z. Cui, *Chem. Mater.* **2001**, *13*, 258.
[24] M. T. Anderson, J. E. Martin, J. G. Odinek, P. P. Newcomer, *Chem. Mater.* **1998**, *10*, 1490.
[25] J. S. Beck, J. C. Vartuli, W. J. Roth, M. E. Leonowicz, C. T. Kresge, K. D. Schmitt, C. T. W. Chu, D. H. Olson, E. W. Sheppard, S. B. Mccullen, J. B. Higgins, J. L. Schlenker, *J. Am. Chem. Soc.* **1992**, *114*, 10834.
[26] S. Huh, J. W. Wiench, J. C. Yoo, M. Pruski, V. S. Y. Lin, *Chem. Mater.* **2003**, *15*, 4247.
[27] S. Huh, J. W. Wiench, B. G. Trewyn, S. Song, M. Pruski, V. S. Y. Lin, *Chem. Commun.* **2003**, 2364.
[28] X. L. Pang, F. Q. Tang, *Micropor. Mesopor. Mat.* **2005**, *85*, 1.
[29] X. L. Huang, L. L. Li, T. L. Liu, N. J. Hao, H. Y. Liu, D. Chen, F. Q. Tang, *ACS Nano* **2011**, *5*, 5390.
[30] V. Alfredsson, M. W. Anderson, *Chem. Mater.* **1996**, *8*, 1141.
[31] F. X. Chen, L. M. Huang, Q. Z. Li, *Chem. Mater.* **1997**, *9*, 2685.
[32] T. W. Kim, P. W. Chung, V. S. Y. Lin, *Chem. Mater.* **2010**, *22*, 5093.
[33] D. Y. Zhao, J. L. Feng, Q. S. Huo, N. Melosh, G. H. Fredrickson, B. F. Chmelka, G. D. Stucky, *Science* **1998**, *279*, 548.

[34] X. L. Ji, K. T. Lee, M. Monjauze, L. F. Nazar, *Chem. Commun.* **2008**, 4288.
[35] Q. J. He, J. L. Shi, J. J. Zhao, Y. Chen, F. Chen, *J. Mater. Chem.* **2009**, *19*, 6498.
[36] Y. Han, J. Y. Ying, *Angew Chem. Int. Edit.* **2005**, *44*, 288.
[37] J. Fan, C. Z. Yu, J. Lei, Q. Zhang, T. C. Li, B. Tu, W. Z. Zhou, D. Y. Zhao, *J. Am. Chem. Soc.* **2005**, *127*, 10795.
[38] X. W. Lou, L. A. Archer, Z. C. Yang, *Adv. Mater.* **2008**, *20*, 3987.
[39] J. Liu, S. Z. Qiao, J. S. Chen, X. W. David Lou, X. Xing, G. Q. Max Lu, *Chem. Commun.* **2011**, *47*, 12578.
[40] G. G. Qi, Y. B. Wang, L. Estevez, A. K. Switzer, X. N. Duan, X. F. Yang, E. P. Giannelis, *Chem. Mater.* **2010**, *22*, 2693.
[41] B. Tan, S. E. Rankin, *Langmuir* **2005**, *21*, 8180.
[42] G. L. Li, G. Liu, E. T. Kang, K. G. Neoh, X. L. Yang, *Langmuir* **2008**, *24*, 9050.
[43] A. M. Javier, O. Kreft, M. Semmling, S. Kempter, A. G. Skirtach, O. T. Bruns, P. del Pino, M. F. Bedard, J. Raedler, J. Käs, C. Plank, G. B. Sukhorukov, W. J. Parak, *Adv. Mater.* **2008**, *20*, 4281.
[44] Y. D. Yin, R. M. Rioux, C. K. Erdonmez, S. Hughes, G. A. Somorjai, A. P. Alivisatos, *Science* **2004**, *304*, 711.
[45] X. W. Lou, C. L. Yuan, E. Rhoades, Q. Zhang, L. A. Archer, *Adv. Funct. Mater.* **2006**, *16*, 1679.
[46] J. Y. Chen, J. M. McLellan, A. Siekkinen, Y. J. Xiong, Z. Y. Li, Y. N. Xia, *J. Am. Chem. Soc.* **2006**, *128*, 14776.
[47] X. J. Wu, D. S. Xu, *J. Am. Chem. Soc.* **2009**, *131*, 2774.
[48] X. J. Wu, D. S. Xu, *Adv. Mater.* **2010**, *22*, 1516.
[49] H. Djojoputro, X. F. Zhou, S. Z. Qiao, L. Z. Wang, C. Z. Yu, G. Q. Lu, *J. Am. Chem. Soc.* **2006**, *128*, 6320.
[50] J. Liu, H. Q. Yang, F. Kleitz, Z. G. Chen, T. Yang, E. Strounina, G. Q. Lu, S. Z. Qiao, *Adv. Funct. Mater.,* DOI: 10.1002/adfm.201101900
[51] J. Liu, S. Z. Qiao, S. B. Hartono, G. Q. Lu, *Angew Chem. Int. Edit.* **2010**, *49*, 4981.
[52] Y. Q. Yeh, B. C. Chen, H. P. Lin, C. Y. Tang, *Langmuir* **2006**, *22*, 6.
[53] J. A. Li, J. Liu, D. H. Wang, R. S. Guo, X. L. Li, W. Qi, *Langmuir* **2010**, *26*, 12267.
[54] Y. S. Lin, S. H. Wu, C. T. Tseng, Y. Hung, C. Chang, C. Y. Mou, *Chem. Commun.* **2009**, 3542.
[55] M. Fujiwara, K. Shiokawa, I. Sakakura, Y. Nakahara, *Nano Lett.* **2006**, *6*, 2925.
[56] Z. G. Feng, Y. S. Li, D. C. Niu, L. Li, W. R. Zhao, H. R. Chen, L. Li, J. H. Gao, M. L. Ruan, J. L. Shi, *Chem. Commun.* **2008**, 2629.
[57] B. Y. Du, Z. Cao, Z. B. Li, A. X. Mei, X. H. Zhang, J. J. Nie, J. T. Xu, Z. Q. Fan, *Langmuir* **2009**, *25*, 12367.
[58] A. Khanal, Y. Inoue, M. Yada, K. Nakashima, *J. Am. Chem. Soc.* **2007**, *129*, 1534.
[59] Q. S. Huo, J. Liu, L. Q. Wang, Y. B. Jiang, T. N. Lambert, E. Fang, *J. Am. Chem. Soc.* **2006**, *128*, 6447.
[60] J. Liu, Q. H. Yang, L. Zhang, H. Q. Yang, J. S. Gao, C. Li, *Chem. Mater.* **2008**, *20*, 4268.
[61] J. Liu, S. Y. Bai, H. Zhong, C. Li, Q. H. Yang, *J. Phys. Chem. C* **2010**, *114*, 953.
[62] D. A. Loy, K. J. Shea, *Chem. Rev.* **1995**, *95*, 1431.
[63] Y. Yang, J. Liu, X. B. Li, X. Liu, Q. H. Yang, *Chem. Mater.* **2011**, *23*, 3676.
[64] M. Roca, A. J. Haes, *J. Am. Chem. Soc.* **2008**, *130*, 14273.
[65] L. L. Li, F. Q. Tang, H. Y. Liu, T. L. Liu, N. J. Hao, D. Chen, X. Teng, J. Q. He, *ACS Nano* **2011**, *5*, 679.
[66] L. F. Tan, D. Chen, H. Y. Liu, F. Q. Tang, *Adv. Mater.* **2010**, *22*, 4885.
[67] H. Y. Liu, D. Chen, L. L. Li, T. L. Liu, L. F. Tan, X. L. Wu, F. Q. Tang, *Angew Chem. Int. Ed.* **2011**, *50*, 891.
[68] Y. Chen, H. R. Chen, D. P. Zeng, Y. B. Tian, F. Chen, J. W. Feng, J. L. Shi, *ACS Nano* **2010**, *4*, 6001.
[69] Y. Chen, H. R. Chen, M. Ma, F. Chen, L. M. Guo, L. X. Zhang, J. L. Shi, *J Mater. Chem.* **2011**, *21*, 5290.
[70] N. Ren, B. Wang, Y. H. Yang, Y. H. Zhang, W. L. Yang, Y. H. Yue, Z. Gao, Y. Tang, *Chem. Mater.* **2005**, *17*, 2582.
[71] T. R. Zhang, J. P. Ge, Y. X. Hu, Q. Zhang, S. Aloni, Y. D. Yin, *Angew Chem. Int. Ed.* **2008**, *47*, 5806.
[72] Q. Zhang, T. R. Zhang, J. P. Ge, Y. D. Yin, *Nano Lett.* **2008**, *8*, 2867.
[73] Q. Zhang, J. P. Ge, J. Goebl, Y. X. Hu, Z. D. Lu, Y. D. Yin, *Nano Res.* **2009**, *2*, 583.
[74] Q. Y. Yu, P. P. Wang, S. Hu, J. F. Hui, J. Zhuang, X. Wang, *Langmuir* **2011**, *27*, 7185.
[75] Y. J. Wong, L. Zhu, W. S. Teo, Y. W. Tan, Y. Yang, C. Wang, H. Chen, *J. Am. Chem. Soc.* **2011**, *133*, 11422.
[76] S. J. Park, Y. J. Kim, S. J. Park, *Langmuir* **2008**, *24*, 12134.
[77] N. Feliu, B. Fadeel, *Nanoscale* **2010**, *2*, 2514.
[78] F. Lu, S. H. Wu, Y. Hung, C. Y. Mou, *Small* **2009**, *5*, 1408.
[79] B. D. Chithrani, A. A. Ghazani, W. C. W. Chan, *Nano Lett.* **2006**, *6*, 662.
[80] F. Osaki, T. Kanamori, S. Sando, T. Sera, Y. Aoyama, *J. Am. Chem. Soc.* **2004**, *126*, 6520.
[81] Q. J. He, Z. W. Zhang, F. Gao, Y. P. Li, J. L. Shi, *Small* **2011**, *7*, 271.
[82] Q. J. He, Z. W. Zhang, Y. Gao, J. L. Shi, Y. P. Li, *Small* **2009**, *5*, 2722.
[83] Y. S. Lin, C. L. Haynes, *J. Am. Chem. Soc.* **2010**, *132*, 4834.
[84] S. P. Hudson, R. F. Padera, R. Langer, D. S. Kohane, *Biomaterials* **2008**, *29*, 4045.
[85] A. Verma, F. Stellacci, *Small* **2010**, *6*, 12.
[86] A. E. Nel, L. Madler, D. Velegol, T. Xia, E. M. V. Hoek, P. Somasundaran, F. Klaessig, V. Castranova, M. Thompson, *Nat. Mater.* **2009**, *8*, 543.
[87] I. I. Slowing, C. W. Wu, J. L. Vivero-Escoto, V. S. Y. Lin, *Small* **2009**, *5*, 57.
[88] F. M. Veronese, G. Pasut, *Drug Discov. Today* **2005**, *10*, 1451.
[89] V. Cauda, C. Argyo, T. Bein, *J. Mater. Chem.* **2010**, *20*, 8693.
[90] Z. M. Tao, B. B. Toms, J. Goodisman, T. Asefa, *Chem. Res. Toxicol.* **2009**, *22*, 1869.
[91] Q. J. He, J. M. Zhang, J. L. Shi, Z. Y. Zhu, L. X. Zhang, W. B. Bu, L. M. Guo, Y. Chen, *Biomaterials* **2010**, *31*, 1085.
[92] H. Hatakeyama, H. Akita, H. Harashima, *Adv. Drug Deliver. Rev.* **2011**, *63*, 152.
[93] T. Ishida, M. Ichihara, X. Wang, K. Yamamoto, J. Kimura, E. Majima, H. Kiwada, *J. Control. Release* **2006**, *112*, 15.
[94] S. M. Moghimi, I. Hamad, *J. Liposome Res.* **2008**, *18*, 195.
[95] I. Slowing, B. G. Trewyn, V. S. Lin, *J. Am. Chem. Soc.* **2006**, *128*, 14792.
[96] S. R. Blumen, K. Cheng, M. E. Ramos-Nino, D. J. Taatjes, D. J. Weiss, C. C. Landry, B. T. Mossman, *Am. J. Resp. Cell Mol. Biol.* **2007**, *36*, 333.
[97] A. J. Di Pasqua, K. K. Sharma, Y. L. Shi, B. B. Toms, W. Ouellette, J. C. Dabrowiak, T. Asefa, *J. Inorg. Biochem.* **2008**, *102*, 1416.
[98] B. S. Chang, J. Guo, C. Y. Liu, J. Qian, W. L. Yang, *J. Mater. Chem.* **2010**, *20*, 9941.
[99] J. S. Souris, C. H. Lee, S. H. Cheng, C. T. Chen, C. S. Yang, J. A. A. Ho, C. Y. Mou, L. W. Lo, *Biomaterials* **2010**, *31*, 5564.
[100] J. W. Liu, A. Stace-Naughton, X. M. Jiang, C. J. Brinker, *J. Am. Chem. Soc.* **2009**, *131*, 1354.
[101] L. S. Wang, L. C. Wu, S. Y. Lu, L. L. Chang, I. T. Teng, C. M. Yang, J. A. A. Ho, *ACS Nano* **2010**, *4*, 4371.
[102] M. M. van Schooneveld, E. Vucic, R. Koole, Y. Zhou, J. Stocks, D. P. Cormode, C. Y. Tang, R. E. Gordon, K. Nicolay, A. Meijerink, Z. A. Fayad, W. J. M. Mulder, *Nano Lett.* **2008**, *8*, 2517.
[103] Y. Yang, W. X. Song, A. H. Wang, P. L. Zhu, J. B. Fei, J. B. Li, *Phys. Chem. Chem. Phys.* **2010**, *12*, 4418.

[104] C. E. Ashley, E. C. Carnes, G. K. Phillips, D. Padilla, P. N. Durfee, P. A. Brown, T. N. Hanna, J. W. Liu, B. Phillips, M. B. Carter, N. J. Carroll, X. M. Jiang, D. R. Dunphy, C. L. Willman, D. N. Petsev, D. G. Evans, A. N. Parikh, B. Chackerian, W. Wharton, D. S. Peabody, C. J. Brinker, *Nat. Mater.* **2011**, *10*, 476.
[105] R. A. Petros, J. M. DeSimone, *Nat. Rev. Drug Discov.* **2010**, *9*, 615.
[106] Y. Geng, P. Dalhaimer, S. S. Cai, R. Tsai, M. Tewari, T. Minko, D. E. Discher, *Nat. Nanotechnol.* **2007**, *2*, 249.
[107] X. L. Huang, X. Teng, D. Chen, F. Q. Tang, J. Q. He, *Biomaterials* **2010**, *31*, 438.
[108] S. Y. Lee, M. Ferrari, P. Decuzzi, *Nanotechnology* **2009**, *20*.
[109] J. A. Champion, S. Mitragotri, *Proc. Natl. Acad. Sci. USA* **2006**, *103*, 4930.
[110] S. Mitragotri, *Pharm. Res.* **2009**, *26*, 232.
[111] H. J. Gao, W. D. Shi, L. B. Freund, *Proc. Natl. Acad. Sci. USA* **2005**, *102*, 9469.
[112] K. Yang, Y. Q. Ma, *Nat. Nanotechnol.* **2010**, *5*, 579.
[113] B. G. Trewyn, J. A. Nieweg, Y. Zhao, V. S. Y. Lin, *Chem. Eng. J.* **2008**, *137*, 23.
[114] Z. M. Tao, B. Toms, J. Goodisman, T. Asefa, *ACS Nano* **2010**, *4*, 789.
[115] H. Meng, S. Yang, Z. X. Li, T. Xia, J. Chen, Z. X. Ji, H. Y. Zhang, X. Wang, S. J. Lin, C. Huang, Z. H. Zhou, J. I. Zink, A. E. Nel, *ACS Nano* **2011**, *5*, 4434.
[116] T. Yu, A. Malugin, H. Ghandehari, *ACS Nano* **2011**, *5*, 5717.
[117] J. H. Park, G. von Maltzahn, L. L. Zhang, M. P. Schwartz, E. Ruoslahti, S. N. Bhatia, M. J. Sailor, *Adv. Mater.* **2008**, *20*, 1630.
[118] V. P. Chauhan, Z. Popovic, O. Chen, J. Cui, D. Fukumura, M. G. Bawendi, R. K. Jain, *Angew Chem. Int. Ed.* **2011**, *50*, 11417.
[119] P. Decuzzi, R. Pasqualini, W. Arap, M. Ferrari, *Pharm. Res.* **2009**, *26*, 235.
[120] A. Nel, T. Xia, L. Mädler, N. Li, *Science* **2006**, *311*, 622.
[121] Z. M. Tao, M. P. Morrow, T. Asefa, K. K. Sharma, C. Duncan, A. Anan, H. S. Penefsky, J. Goodisman, A. K. Souid, *Nano Lett.* **2008**, *8*, 1517.
[122] H. J. Eom, J. Choi, *Toxicol. In Vitro* **2009**, *23*, 1326.
[123] S. Lee, H. S. Yun, S. H. Kim, *Biomaterials* **2011**, *32*, 9434.
[124] M. A. Maurer-Jones, Y. S. Lin, C. L. Haynes, *ACS Nano* **2010**, *4*, 3363.
[125] Q. J. He, J. L. Shi, M. Zhu, Y. Chen, F. Chen, *Micropor. Mesopor. Mat.* **2010**, *131*, 314.
[126] N. Doshi, B. Prabhakarpandian, A. Rea-Ramsey, K. Pant, S. Sundaram, S. Mitragotri, *J. Control. Release* **2010**, *146*, 196.
[127] T. L. Liu, L. L. Li, X. Teng, X. L. Huang, H. Y. Liu, D. Chen, J. Ren, J. Q. He, F. Q. Tang, *Biomaterials* **2011**, *32*, 1657.
[128] E. Burello, A. Worth, *Nat. Nanotechnol.* **2011**, *6*, 138.
[129] R. A. Siegel, J. Kost, R. Langer, *J. Control. Release* **1989**, *8*, 223.
[130] T. Lebold, C. Jung, J. Michaelis, C. Brauchle, *Nano Lett.* **2009**, *9*, 2877.
[131] L. Zhang, S. Z. Qiao, Y. G. Jin, L. N. Cheng, Z. F. Yan, G. Q. Lu, *Adv. Funct. Mater.* **2008**, *18*, 3834.
[132] F. Balas, M. Manzano, M. Colilla, M. Vallet-Regí, *Acta Biomater.* **2008**, *4*, 514.
[133] H. H. P. Yiu, C. H. Botting, N. P. Botting, P. A. Wright, *Phys. Chem. Chem. Phys.* **2001**, *3*, 2983.
[134] M. Vallet-Regí, F. Balas, M. Colilla, M. Manzano, *Prog. Solid State Chem.* **2008**, *36*, 163.
[135] P. Horcajada, A. Ramila, J. Perez-Pariente, M. Vallet-Regí, *Micropor. Mesopor. Mat.* **2004**, *68*, 105.
[136] F. Balas, M. Manzano, P. Horcajada, M. Vallet-Regí, *J. Am. Chem. Soc.* **2006**, *128*, 8116.
[137] B. Muñoz, A. Rámila, J. Pérez-Pariente, I. Díaz, M. Vallet-Regí, *Chem. Mater.* **2003**, *15*, 500.
[138] J. L. Gu, S. S. Su, Y. S. Li, Q. J. He, F. Y. Zhong, J. L. Shi, *J. Phys. Chem. Lett.* **2010**, *1*, 3446.
[139] A. M. Chen, M. Zhang, D. G. Wei, D. Stueber, O. Taratula, T. Minko, H. X. He, *Small* **2009**, *5*, 2673.
[140] J. Lu, M. Liong, J. I. Zink, F. Tamanoi, *Small* **2007**, *3*, 1341.
[141] A. Nieto, F. Balas, M. Colilla, M. Manzano, M. Vallet-Regí, *Micropor. Mesopor. Mat.* **2008**, *116*, 4.
[142] R. Mellaerts, R. Mols, J. A. G. Jammaer, C. A. Aerts, P. Annaert, J. Van Humbeeck, G. Van den Mooter, P. Augustijns, J. A. Martens, *Eur. J. Pharm. Biopharm.* **2008**, *69*, 223.
[143] A. MaHam, Z. W. Tang, H. Wu, J. Wang, Y. H. Lin, *Small* **2009**, *5*, 1706.
[144] A. Sood, R. Panchagnula, *Chem. Rev.* **2001**, *101*, 3275.
[145] S. Hudson, J. Cooney, E. Magner, *Angew Chem. Int. Edit.* **2008**, *47*, 8582.
[146] T. P. B. Nguyen, J. W. Lee, W. G. Shim, H. Moon, *Micropor. Mesopor. Mat.* **2008**, *110*, 560.
[147] J. Zhang, L. M. Postovit, D. S. Wang, R. B. Gardiner, R. Harris, M. M. Abdul, A. A. Thomas, *Nanoscale Res. Lett.* **2009**, *4*, 1297.
[148] I. I. Slowing, B. G. Trewyn, V. S. Y. Lin, *J. Am. Chem. Soc.* **2007**, *129*, 8845.
[149] F. Torney, B. G. Trewyn, V. S. Y. Lin, K. Wang, *Nat. Nanotechnol.* **2007**, *2*, 295.
[150] D. R. Radu, C. Y. Lai, K. Jeftinija, E. W. Rowe, S. Jeftinija, V. S. Y. Lin, *J. Am. Chem. Soc.* **2004**, *126*, 13216.
[151] C. Hom, J. Lu, M. Liong, H. Z. Luo, Z. X. Li, J. I. Zink, F. Tamanoi, *Small* **2010**, *6*, 1185.
[152] I. Y. Park, I. Y. Kim, M. K. Yoo, Y. J. Choi, M. H. Cho, C. S. Cho, *Int. J. Pharm.* **2008**, *359*, 280.
[153] T. A. Xia, M. Kovochich, M. Liong, H. Meng, S. Kabehie, S. George, J. I. Zink, A. E. Nel, *ACS Nano* **2009**, *3*, 3273.
[154] F. Gao, P. Botella, A. Corma, J. Blesa, L. Dong, *J. Phys. Chem. B* **2009**, *113*, 1796.
[155] M. H. Kim, H. K. Na, Y. K. Kim, S. R. Ryoo, H. S. Cho, K. E. Lee, H. Jeon, R. Ryoo, D. H. Min, *ACS Nano* **2011**, *5*, 3568.
[156] X. Li, Q. R. Xie, J. X. Zhang, W. L. Xia, H. C. Gu, *Biomaterials* **2011**, *32*, 9546.
[157] X. Li, J. X. Zhang, H. C. Gu, *Langmuir* **2011**, *27*, 6099.
[158] S. R. Bhattarai, E. Muthuswamy, A. Wani, M. Brichacek, A. L. Castaneda, S. L. Brock, D. Oupicky, *Pharm. Res.* **2010**, *27*, 2556.
[159] Y. F. Zhu, T. Ikoma, N. Hanagata, S. Kaskel, *Small* **2010**, *6*, 471.
[160] Y. F. Zhu, W. J. Meng, H. Gao, N. Hanagata, *J Phys Chem C* **2011**, *115*, 13630.
[161] N. K. Mal, M. Fujiwara, Y. Tanaka, *Nature* **2003**, *421*, 350.
[162] Q. N. Lin, Q. Huang, C. Y. Li, C. Y. Bao, Z. Z. Liu, F. Y. Li, L. Y. Zhu, *J. Am. Chem. Soc.* **2010**, *132*, 10645.
[163] J. L. Vivero-Escoto, I. I. Slowing, C. W. Wu, V. S. Y. Lin, *J. Am. Chem. Soc.* **2009**, *131*, 3462.
[164] S. Angelos, E. Choi, F. Vogtle, L. De Cola, J. I. Zink, *J. Phys. Chem. C* **2007**, *111*, 6589.
[165] Y. C. Zhu, M. Fujiwara, *Angew Chem. Int. Edit.* **2007**, *46*, 2241.
[166] T. D. Nguyen, K. C. F. Leung, M. Liong, Y. Liu, J. F. Stoddart, J. I. Zink, *Adv. Funct. Mater.* **2007**, *17*, 2101.
[167] C. Y. Lai, B. G. Trewyn, D. M. Jeftinija, K. Jeftinija, S. Xu, S. Jeftinija, V. S. Y. Lin, *J. Am. Chem. Soc.* **2003**, *125*, 4451.
[168] S. Giri, B. G. Trewyn, M. P. Stellmaker, V. S. Y. Lin, *Angew Chem. Int. Edit.* **2005**, *44*, 5038.
[169] H. Kim, S. Kim, C. Park, H. Lee, H. J. Park, C. Kim, *Adv. Mater.* **2010**, *22*, 4280.
[170] E. Climent, R. Martinez-Manez, F. Sancenon, M. D. Marcos, J. Soto, A. Maquieira, P. Amoros, *Angew Chem. Int. Edit.* **2010**, *49*, 7281.
[171] C. L. Zhu, C. H. Lu, X. Y. Song, H. H. Yang, X. R. Wang, *J. Am. Chem. Soc.* **2011**, *133*, 1278.

[172] C. Park, K. Oh, S. C. Lee, C. Kim, *Angew Chem. Int. Ed.* **2007**, *46*, 1455.
[173] S. Angelos, N. M. Khashab, Y. W. Yang, A. Trabolsi, H. A. Khatib, J. F. Stoddart, J. I. Zink, *J. Am. Chem. Soc.* **2009**, *131*, 12912.
[174] A. Schlossbauer, C. Dohmen, D. Schaffert, E. Wagner, T. Bein, *Angew Chem. Int. Ed.* **2011**, *50*, 6828.
[175] S. Angelos, Y. W. Yang, K. Patel, J. F. Stoddart, J. I. Zink, *Angew Chem. Int. Ed.* **2008**, *47*, 2222.
[176] F. Muharnmad, M. Y. Guo, W. X. Qi, F. X. Sun, A. F. Wang, Y. J. Guo, G. S. Zhu, *J. Am. Chem. Soc.* **2011**, *133*, 8778.
[177] X. F. Zhang, L. Clime, H. Roberge, F. Normandin, L. Yahia, E. Sacher, T. Veres, *J. Phys. Chem. C* **2011**, *115*, 1436.
[178] C. Y. Liu, J. Guo, W. L. Yang, J. H. Hu, C. C. Wang, S. K. Fu, *J. Mater. Chem.* **2009**, *19*, 4764.
[179] P. W. Chung, R. Kumar, M. Pruski, V. S. Y. Lin, *Adv. Funct. Mater.* **2008**, *18*, 1390.
[180] X. J. Wan, D. Wang, S. Y. Liu, *Langmuir* **2010**, *26*, 15574.
[181] R. Liu, X. Zhao, T. Wu, P. Y. Feng, *J. Am. Chem. Soc.* **2008**, *130*, 14418.
[182] Z. Luo, K. Y. Cai, Y. Hu, L. Zhao, P. Liu, L. Duan, W. H. Yang, *Angew Chem. Int. Ed.* **2011**, *50*, 640.
[183] A. M. Sauer, A. Schlossbauer, N. Ruthardt, V. Cauda, T. Bein, C. Bräuchle, *Nano Lett.* **2010**, *10*, 3684.
[184] S. H. Hu, T. Y. Liu, H. Y. Huang, D. M. Liu, S. Y. Chen, *Langmuir* **2008**, *24*, 239.
[185] Y. C. Zhu, H. J. Liu, F. Li, Q. C. Ruan, H. Wang, M. Fujiwara, L. Z. Wang, G. Q. Lu, *J. Am. Chem. Soc.* **2010**, *132*, 1450.
[186] A. Schlossbauer, J. Kecht, T. Bein, *Angew Chem. Int. Ed.* **2009**, *48*, 3092.
[187] A. Bernardos, E. Aznar, M. D. Marcos, R. Martinez-Manez, F. Sancenon, J. Soto, J. M. Barat, P. Amoros, *Angew Chem. Int. Ed.* **2009**, *48*, 5884.
[188] A. Bernardos, L. Mondragon, E. Aznar, M. D. Marcos, R. Martinez-Manez, F. Sancenon, J. Soto, J. M. Barat, E. Perez-Paya, C. Guillem, P. Amoros, *ACS Nano* **2010**, *4*, 6353.
[189] Y. Itoh, M. Matsusaki, T. Kida, M. Akashi, *Biomacromolecules* **2006**, *7*, 2715.
[190] K. Patel, S. Angelos, W. R. Dichtel, A. Coskun, Y. W. Yang, J. I. Zink, J. F. Stoddart, *J. Am. Chem. Soc.* **2008**, *130*, 2382.
[191] R. Liu, Y. Zhang, P. Y. Feng, *J. Am. Chem. Soc.* **2009**, *131*, 15128.
[192] N. M. Khashab, A. Trabolsi, Y. A. Lau, M. W. Ambrogio, D. C. Friedman, H. A. Khatib, J. I. Zink, J. F. Stoddart, *Eur. J. Org. Chem.* **2009**, 1669.
[193] E. Aznar, M. D. Marcos, R. Martinez-Manez, F. Sancenon, J. Soto, P. Amoros, C. Guillem, *J. Am. Chem. Soc.* **2009**, *131*, 6833.
[194] H. A. Meng, M. Xue, T. A. Xia, Y. L. Zhao, F. Tamanoi, J. F. Stoddart, J. I. Zink, A. E. Nel, *J. Am. Chem. Soc.* **2010**, *132*, 12690.
[195] J. Lu, E. Choi, F. Tamanoi, J. I. Zink, *Small* **2008**, *4*, 421.
[196] H. P. Rim, K. H. Min, H. J. Lee, S. Y. Jeong, S. C. Lee, *Angew Chem. Int. Ed.* **2011**, *50*, 8853.
[197] Z. Z. Li, L. X. Wen, L. Shao, J. F. Chen, *J. Control. Release* **2004**, *98*, 245.
[198] J. F. Chen, H. M. Ding, J. X. Wang, L. Shao, *Biomaterials* **2004**, *25*, 723.
[199] Y. F. Zhu, J. L. Shi, H. R. Chen, W. H. Shen, X. P. Dong, *Micropor. Mesopor. Mat.* **2005**, *84*, 218.
[200] N. E. Botterhuis, Q. Y. Sun, P. C. M. M. Magusin, R. A. van Santen, N. A. J. M. Sommerdijk, *Chem. Eur. J.* **2006**, *12*, 1448.
[201] W. R. Zhao, H. R. Chen, Y. S. Li, L. Li, M. D. Lang, J. L. Shi, *Adv. Funct. Mater.* **2008**, *18*, 2780.
[202] C. X. Lin, S. Z. Qiao, C. Z. Yu, S. Ismadji, G. Q. Lu, *Micropor. Mesopor. Mat.* **2009**, *117*, 213.
[203] C. L. Wu, X. Wang, L. Z. Zhao, Y. H. Gao, R. J. Ma, Y. L. An, L. Q. Shi, *Langmuir* **2010**, *26*, 18503.
[204] S. Tan, Q. X. Wu, J. Wang, Y. L. Wang, X. L. Liu, K. K. Sui, X. Y. Deng, H. F. Wang, M. H. Wu, *Micropor. Mesopor. Mat.* **2011**, *142*, 601.
[205] Y. Zhao, L. N. Lin, Y. Lu, S. F. Chen, L. A. Dong, S. H. Yu, *Adv. Mater.* **2010**, *22*, 5255.
[206] X. M. Jiang, T. L. Ward, Y. S. Cheng, J. W. Liu, C. J. Brinker, *Chem. Commun.* **2010**, *46*, 3019.
[207] T. T. Wang, F. Chai, Q. Fu, L. Y. Zhang, H. Y. Liu, L. Li, Y. Liao, Z. M. Su, C. A. Wang, B. Y. Duan, D. X. Ren, *J. Mater. Chem.* **2011**, *21*, 5299.
[208] C. C. Huang, W. Huang, C. S. Yeh, *Biomaterials* **2011**, *32*, 556.
[209] D. Chen, L. L. Li, F. Q. Tang, S. O. Qi, *Adv. Mater.* **2009**, *21*, 3804.
[210] L. L. Li, Y. Q. Guan, H. Y. Liu, N. J. Hao, T. L. Liu, X. W. Meng, C. H. Fu, Y. Z. Li, Q. L. Qu, Y. G. Zhang, S. Y. Ji, L. Chen, D. Chen, F. Q. Tang, *ACS Nano* **2011**, *5*, 7462.
[211] Y. F. Zhu, J. L. Shi, W. H. Shen, X. P. Dong, J. W. Feng, M. L. Ruan, Y. S. Li, *Angew Chem. Int. Edit.* **2005**, *44*, 5083.
[212] L. Du, S. J. Liao, H. A. Khatib, J. F. Stoddart, J. I. Zink, *J. Am. Chem. Soc.* **2009**, *131*, 15136.
[213] Z. W. Deng, Z. P. Zhen, X. X. Hu, S. L. Wu, Z. S. Xu, P. K. Chu, *Biomaterials* **2011**, *32*, 4976.
[214] A. Jemal, F. Bray, M. M. Center, J. Ferlay, E. Ward, D. Forman, *Ca-Cancer J. Clin.* **2011**, *61*, 69.
[215] M. E. Davis, Z. Chen, D. M. Shin, *Nat. Rev. Drug Discov.* **2008**, *7*, 771.
[216] S. M. Moghimi, A. C. Hunter, J. C. Murray, *Pharmacol. Rev.* **2001**, *53*, 283.
[217] M. Longmire, P. L. Choyke, H. Kobayashi, *Nanomedicine-UK* **2008**, *3*, 703.
[218] P. Vaupel, F. Kallinowski, P. Okunieff, *Cancer Res.* **1989**, *49*, 6449.
[219] B. Kim, G. Han, B. J. Toley, C. K. Kim, V. M. Rotello, N. S. Forbes, *Nat. Nanotechnol.* **2010**, *5*, 465.
[220] T. R. Daniels, T. Delgado, G. Helguera, M. L. Penichet, *Clin. Immunol.* **2006**, *121*, 159.
[221] X. H. Huang, X. H. Peng, Y. Q. Wang, Y. X. Wang, D. M. Shin, M. A. El-Sayed, S. M. Nie, *ACS Nano* **2011**, *5*, 6765.
[222] T. G. Iversen, T. Skotland, K. Sandvig, *Nano Today* **2011**, *6*, 176.
[223] C. Barbé, J. Bartlett, L. G. Kong, K. Finnie, H. Q. Lin, M. Larkin, S. Calleja, A. Bush, G. Calleja, *Adv. Mater.* **2004**, *16*, 1959.
[224] H. Meng, M. Xue, T. Xia, Z. X. Ji, D. Y. Tarn, J. I. Zink, A. E. Nel, *ACS Nano* **2011**, *5*, 4131.
[225] H. K. de Wolf, C. J. Snel, F. J. Verbaan, R. M. Schiffelers, W. E. Hennink, G. Storm, *Int. J. Pharm.* **2007**, *331*, 167.
[226] F. J. Verbaan, C. Oussoren, C. J. Snel, D. J. A. Crommelin, W. E. Hennink, G. Storm, *J. Gene Med.* **2004**, *6*, 64.
[227] J. M. Rosenholm, E. Peuhu, L. T. Bate-Eya, J. E. Eriksson, C. Sahlgren, M. Lindén, *Small* **2010**, *6*, 1234.
[228] J. Lu, Z. Li, J. I. Zink, F. Tamanoi, *Nanomedicine-UK* DOI: 10.1016/j.nano.2011.06.002
[229] J. M. Rosenholm, E. Peuhu, J. E. Eriksson, C. Sahlgren, M. Lindén, *Nano Lett.* **2009**, *9*, 3308.
[230] J. M. Rosenholm, A. Meinander, E. Peuhu, R. Niemi, J. E. Eriksson, C. Sahlgren, M. Lindén, *ACS Nano* **2009**, *3*, 197.
[231] D. P. Ferris, J. Lu, C. Gothard, R. Yanes, C. R. Thomas, J. C. Olsen, J. F. Stoddart, F. Tamanoi, J. I. Zink, *Small* **2011**, *7*, 1816.
[232] C. L. Zhu, X. Y. Song, W. H. Zhou, H. H. Yang, Y. H. Wen, X. R. Wang, *J Mater. Chem.* **2009**, *19*, 7765.
[233] C. P. Tsai, C. Y. Chen, Y. Hung, F. H. Chang, C. Y. Mou, *J. Mater. Chem.* **2009**, *19*, 5737.
[234] J. Lu, M. Liong, S. Sherman, T. Xia, M. Kovochich, A. E. Nel, J. I. Zink, F. Tamanoi, *Nanobiotechnol.* **2007**, *3*, 89.
[235] L. Li, Y. Guan, H. Liu, N. Hao, T. Liu, X. Meng, C. Fu, Y. Li, Q. Qu, Y. Zhang, S. Ji, L. Chen, D. Chen, F. Tang, *ACS Nano* **2011**, *5*, 7462.

[236] A. Nakamizo, F. Marini, T. Amano, A. Khan, M. Studeny, J. Gumin, J. Chen, S. Hentschel, G. Vecil, J. Dembinski, M. Andreeff, F. F. Lang, *Cancer Res.* **2005**, *65*, 3307.
[237] M. M. Gottesman, T. Fojo, S. E. Bates, *Nat. Rev. Cancer* **2002**, *2*, 48.
[238] M. Dean, T. Fojo, S. Bates, *Nat. Rev. Cancer* **2005**, *5*, 275.
[239] D. Hanahan, R. A. Weinberg, *Cell* **2011**, *144*, 646.
[240] A. Shapira, Y. D. Livney, H. J. Broxterman, Y. G. Assaraf, *Drug Resist. Update.* **2011**, *14*, 150.
[241] A. Abdollahi, J. Folkman, *Drug Resist. Update.* **2010**, *13*, 16.
[242] H. Meng, M. Liong, T. Xia, Z. Li, Z. Ji, J. I. Zink, A. E. Nel, *ACS Nano* **2010**, *4*, 4539.
[243] Q. He, Y. Gao, L. Zhang, Z. Zhang, F. Gao, X. Ji, Y. Li, J. Shi, *Biomaterials* **2011**, *32*, 7711.
[244] P. Ranganathan, K. L. Weaver, A. J. Capobianco, *Nat. Rev. Cancer* **2011**, *11*, 338.
[245] V. Mamaeva, J. M. Rosenholm, L. T. Bate-Eya, L. Bergman, E. Peuhu, A. Duchanoy, L. E. Fortelius, S. Landor, D. M. Toivola, M. Lindén, C. Sahlgren, *Mol. Ther.* **2011**, *19*, 1538.
[246] A. Guerrero-Martínez, J. Pérez-Juste, L. M. Liz-Marzán, *Adv. Mater.* **2010**, *22*, 1182.
[247] S. H. Wu, Y. S. Lin, Y. Hung, Y. H. Chou, Y. H. Hsu, C. Chang, C. Y. Mou, *ChemBioChem* **2008**, *9*, 53.
[248] C. P. Tsai, Y. Hung, Y. H. Chou, D. M. Huang, J. K. Hsiao, C. Chang, Y. C. Chen, C. Y. Mou, *Small* **2008**, *4*, 186.
[249] J. Kim, J. E. Lee, J. Lee, J. H. Yu, B. C. Kim, K. An, Y. Hwang, C. H. Shin, J. G. Park, J. Kim, T. Hyeon, *J. Am. Chem. Soc.* **2006**, *128*, 688.
[250] M. Liong, J. Lu, M. Kovochich, T. Xia, S. G. Ruehm, A. E. Nel, F. Tamanoi, J. I. Zink, *ACS Nano* **2008**, *2*, 889.
[251] Y. S. Lin, C. L. Haynes, *Chem. Mater.* **2009**, *21*, 3979.
[252] H. H. P. Yiu, H. J. Niu, E. Biermans, G. van Tendeloo, M. J. Rosseinsky, *Adv. Funct. Mater.* **2010**, *20*, 1599.
[253] J. E. Lee, N. Lee, H. Kim, J. Kim, S. H. Choi, J. H. Kim, T. Kim, I. C. Song, S. P. Park, W. K. Moon, T. Hyeon, *J. Am. Chem. Soc.* **2010**, *132*, 552.
[254] J. Liu, B. Wang, S. B. Hartono, T. Liu, P. Kantharidis, A. P. Middelberg, G. Q. Lu, L. He, S. Z. Qiao, *Biomaterials.* **2012**, *33*, 970.
[255] J. Liu, S. Z. Qiao, Q. H. Hu, G. Q. Lu, *Small* **2011**, *7*, 425.
[256] Y. S. Lin, S. H. Wu, Y. Hung, Y. H. Chou, C. Chang, M. L. Lin, C. P. Tsai, C. Y. Mou, *Chem. Mater.* **2006**, *18*, 5170.
[257] L. Sun, Y. Zang, M. D. Sun, H. G. Wang, X. J. Zhu, S. F. Xu, Q. B. Yang, Y. X. Li, Y. M. Shan, *J. Colloid Interf. Sci.* **2010**, *350*, 90.
[258] S. H. Cheng, C. H. Lee, M. C. Chen, J. S. Souris, F. G. Tseng, C. S. Yang, C. Y. Mou, C. T. Chen, L. W. Lo, *J. Mater. Chem.* **2010**, *20*, 6149.
[259] P. J. Chen, S. H. Hu, C. S. Hsiao, Y. Y. Chen, D. M. Liu, S. Y. Chen, *J. Mater. Chem.* **2011**, *21*, 2535.
[260] J. Kim, H. S. Kim, N. Lee, T. Kim, H. Kim, T. Yu, I. C. Song, W. K. Moon, T. Hyeon, *Angew Chem. Int. Edit.* **2008**, *47*, 8438.
[261] F. Wang, X. L. Chen, Z. X. Zhao, S. H. Tang, X. Q. Huang, C. H. Lin, C. B. Cai, N. F. Zheng, *J. Mater. Chem.* **2011**, *21*, 11244.
[262] Y. Chen, H. R. Chen, S. J. Zhang, F. Chen, L. X. Zhang, J. M. Zhang, M. Zhu, H. X. Wu, L. M. Guo, J. W. Feng, J. L. Shi, *Adv. Funct. Mater.* **2011**, *21*, 270.
[263] L. R. Hirsch, R. J. Stafford, J. A. Bankson, S. R. Sershen, B. Rivera, R. E. Price, J. D. Hazle, N. J. Halas, J. L. West, *P. Natl. Acad. Sci. USA* **2003**, *100*, 13549.
[264] H. Y. Liu, T. L. Liu, X. L. Wu, L. L. Li, L. F. Tan, D. Chen, F. Q. Tang, *Adv. Mater.* DOI: 10.1002/adma.201103343.
[265] K. Yamashita, Y. Yoshioka, K. Higashisaka, K. Mimura, Y. Morishita, M. Nozaki, T. Yoshida, T. Ogura, H. Nabeshi, K. Nagano, Y. Abe, H. Kamada, Y. Monobe, T. Imazawa, H. Aoshima, K. Shishido, Y. Kawai, T. Mayumi, S. Tsunoda, N. Itoh, T. Yoshikawa, I. Yanagihara, S. Saito, Y. Tsutsumi, *Nat. Nanotechnol.* **2011**, *6*, 321.
[266] M. Benezra, O. Penate-Medina, P. B. Zanzonico, D. Schaer, H. Ow, A. Burns, E. DeStanchina, V. Longo, E. Herz, S. Iyer, J. Wolchok, S. M. Larson, U. Wiesner, M. S. Bradbury, *J. Clin. Invest.* **2011**, *121*, 2768.
[267] R. Friedman, *J. Natl. Cancer Inst.* **2011**, *103*, 1428.